Materials Advances

ROYAL SOCIETY OF CHEMISTRY

REVIEW

View Article Online
View Journal | View Issue



Cite this: *Mater. Adv.*, 2025, 6, 84

# Achievements, challenges, and stability of layer double hydroxide and carbon nanotube hybrid electrode materials for clean and sustainable energy storage supercapacitor application: an extensive review

Priyadarshi K. Ray and Kulamani Parida *

Considering the massive environmental concerns due to air and water pollution, exhaustion of natural sources and global warming, awareness of environmental protection is required. In this case, a disruptive method to develop sustainable energy storage systems in the form of electrochemical energy storage (EES) devices is urgent. Supercapacitors or ultracapacitors are one the best long-standing passive electronic devices that can deliver maximum power and energy density. Accordingly, in the energy field, there has been increasing interest in their charging/discharging power, with research focusing on their cost, environmental friendliness, toxicity, portability, safety, service life, and disposal. Significant research has been conducted on layered double hydroxide (LDH) and carbon nanotube (CNT) composites for the design and fabrication of electrodes, with a focus on electrolyte operating window potential and cell temperature. The aim of this review is to highlight the extraordinary properties of supercapacitors (SCs) in terms of their physical, chemical and electrochemical performances. Importantly, this review offers insights into some of the key LDH/CNT nanocomposite SC electrodes. The fundamental storage mechanism, advantages and drawbacks of LDH/CNT composites together with their popularity, physicochemical techniques, applications, environmental conditions, challenges and future perspectives are elaborated. We hope that this review will encourage the research community and will enhance the results with comparative challenges.

Received 31st July 2024,
Accepted 15th November 2024

DOI: 10.1039/d4ma00772g

rsc.li/materials-advances



## 1. Introduction

Severe environmental pollution, global warming, and depletion of fossil resources have raised several concerns. Moreover, the widespread usage of natural resources (fossil fuels) is a critical environmental problem because it generates pollutants in the form of greenhouse gases and dust particles during the production of energy.[1–4] To date, energy storage is limited, but there is a drastic increase in the population and essential needs. Therefore, researchers have found a green energy storage solution that is safe for the environment and a practical way to store electrical energy called supercapacitors or electrochemical capacitors. These passive devices have attracted interest globally to optimize their properties and characteristics owing to their limitless usage in electric vehicles (motorcycles, buses, *etc.*), aircraft, UPSs, cell phones, and medical devices.[5] ESSs, *viz.* batteries,[6,7] capacitors, and supercapacitors, are critical for maintaining and storing sustainable and renewable energy sources. In addition, their conversion plays an essential role in our daily lives. Secondary batteries, capacitors, fuel cells, and supercapacitors are the foremost ESSs for utilization in terms of their two basic properties of energy density and power density. Batteries are undoubtedly superior considering their energy density, especially lithium-ion batteries (LiBs), which store energy through electrochemical intercalation reactions of ions in a slow diffusion process in solid active electrode materials.[8] Generally, LiBs are composed of a graphite anode and lithium oxide-based metal as the cathode, leading to low power density (nearly 500–2000 W $kg^{-1}$)[9] because charge/discharge is limited by lithium-ion diffusion during phase transformation. Furthermore, LiBs have other drawbacks: low power density, short life cycle, poor electrochemical durability as well as longevity and safety concerns.[10] Thus, to overcome these difficulties, SCs are considered the most accurate, soft, implantable power supplies favoring high energy required devices, as

*Centre for Nano Science and Nano Technology, Institute of Technical Education and Research (ITER), Siksha 'O' Anusandhan Deemed to be University, Bhubaneswar-751030, Odisha, India. E-mail: kulamaniparida@soauniversity.ac.in, paridakulamani@yahoo.com*

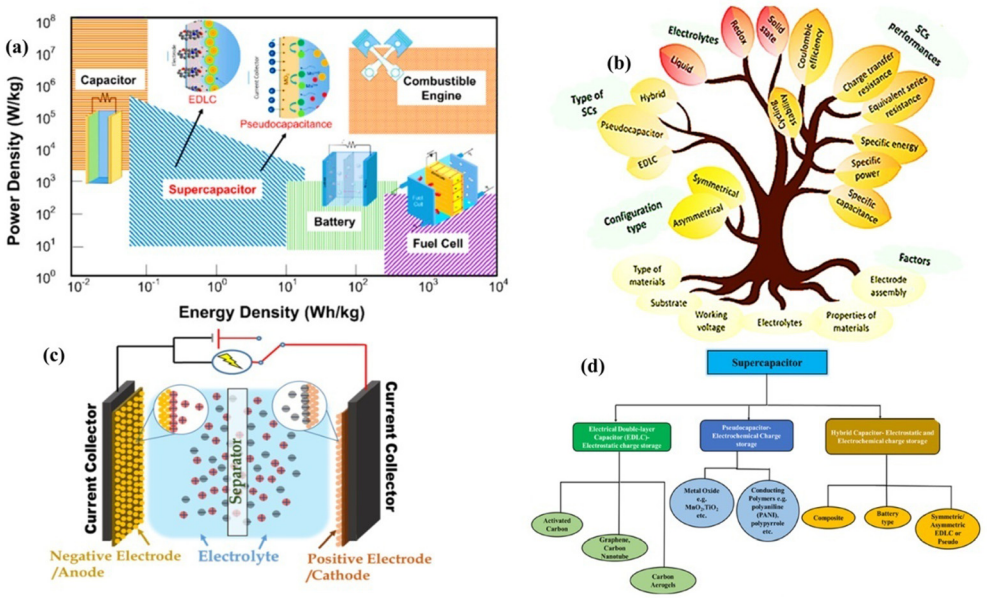


Fig. 1 (a) Ragone plot for various energy storage devices. Reproduced with permission from ref. 5. (b) Types, electrolytes, and factors affecting the performance of supercapacitors. Reproduced with permission from ref. 21. (c) Schematic view of the charge storage in SCs. Reproduced with permission from ref. 5. (d) Classification of SCs based on their storage mechanism. Reproduced with permission from ref. 12.

shown in the Ragone plot of energy density *vs.* power density in Fig. 1(a). According to this graph, SCs have high power capability and relatively large energy density[11–13] in comparison with conventional dielectric capacitors,[14] where energy density is a crucial parameter in the energy storage-conversion-delivery chain for an instant burst of power in these innovative storage devices.[15] Moreover, SCs possess better properties of a long life cycle, wide potential window, better cycle stability, sustainability, and wide operating temperature with low cost, easy maintenance, and zero pollution than both fuel cells and capacitors[16–18] and LiBs. In contrast, they have a very low energy density.[19] Therefore, the research on SCs is stimulated by their unique properties. Further, SCs can be achieved by improving the active materials at the electrodes and achieving a high surface area, pore size distribution, stability, and better capacitance retention after a long charge–discharge cycle.[20] Besides these properties, Strandberg-type polyoxometalate cluster-based coordination polymers containing organophosphorus as the central unit show enormous hidden potential including high electron density, controllable size, catalytic active sites, unique microstructure and excellent electronic conductivity for supercapacitor performance and practical applications in molecular electronics. Thus, SCs will play vital role in realizing economic growth, decreasing harmful emissions and greenhouse gases, and reducing the dependency on diesel fuel.

Moreover, unlike conventional capacitors, SCs are not composed of dielectric material. They have three basic components including active material electrodes installed in the desired electrolyte through a mechanical separator to enhance the electrolytic ion diffusion into the electrode and prevent short circuits in solution. The ''current collector'' collects conducting electric current from the electrodes to power sources.[22–24] Accordingly, a research prospect is to develop cutting-edge energy conversion and storage technologies based on advanced materials with distinct and extraordinary properties. Therefore, the research community has focused on finding the best active electrode materials, which will simultaneously play other roles in the fabrication of smooth and robust hybrid SCs by driving the development of materials including carbonaceous materials [carbon quantum dots, activated carbon, carbon aero-gel, graphene, CNTs, graphene oxide, and rGO], layered double hydroxides (transition metal oxide LDHs),[25] and MXenes.[26] Among them, single-walled carbon nanotubes (SWCNTs) and multiwalled carbon nanotubes (MWCNTs) are promising. MWCNTs are one-dimensional materials composed of several concentric layers of graphene, which possess high electrical and thermal conductivity, good mechanical strength, high specific surface area and the highest specific capacitance. Alternatively, LDHs show unique 3D hierarchical porous structural attributes, good stability, optimized conductivity and feasible and experimental features for pseudocapacitance, which are essential for high-performance supercapacitors. Accordingly, composites of these materials possess the activity of their components, which can be widely used as electrode materials for supercapacitors. Mesopores and micropores are created at the boundary between composite electrodes and the electrolyte during the electrochemical synthesis process, which strongly enhance the transport of ions/electrons for energy storage. This is because of the vast redox active sites and stability of electrodes. Secondly, MWCNTs prevent agglomeration and enhance the electrode–electrolyte accessibility. The main exciting feature to be analyzed is the development of materials having a better energy density than batteries or fuel cells without hampering their other essential properties.

In this review, we provide a detailed overview of the performance of LDH and CNT composite architecture materials for supercapacitor applications due to the growing energy demand and their environmentally friendly nature, low cost, easy manufacturing process, excellent electrochemical activity, morphology depending on their synthesis process, stability during redox reactions, capacity to change their shape and size, and wide operating temperature range. Many reviews in the literature show the efficacy in developing very stable electrode materials for potential future storage strategies, especially these composites. Additionally, the porosity of composites will increase the number of reactive sites, which will create surplus ions that may be kept at the collector current and further induce the doping or modification of different elements or compounds. As a result, the microscopic perspective of structure enables the design of novel derived composites. By using the above-mentioned helpful concepts of LDH/CNT asymmetric SCs as the most suitable properties, readers should concentrate on obtaining basic properties such as storage of maximum charges, fast charging/discharging rate, high degree of crystallinity, cycling stability, retention rate, and both high energy and power density. A bird's-eye view of LDH/CNT composites is highlighted by this thorough analysis.

To date, although many articles have been published on this topic, bridging the gap between recent progress is still required. Hence, we provide an up-to-date overview and summarize the various trends of LDH/CNT composites and their application in the SC field. This is because both LDHs and CNTs have excellent physical and chemical properties as bulk or nanocomposites.[27] CNTs play a leading role in a myriad of applications including electrocatalysis, micro and nanoelectronics, and flexible energy capacity building devices, and their use in the formation of composites is due to their large surface area, good conductivity, cost-effectiveness, excellent mechanical strength, and heat tolerance.[28] When they are combined with materials with high mechanical strength, accessible materials with potential for ion/charge production will be obtained, which will be ideal for the fabrication of energy storage devices.[29] Therefore, this review is comprised of sections discussing the evolution of electrode materials and their composites (positive, negative, and both), fundamental of SCs and their types and factors influencing their performance, as shown in Fig. 1(b). Also, their physicochemical and thermodynamic properties, different types of synthesis and characterization, commercial applications and high-temperature stability, which is a significant operating factor for space and military applications, are discussed.[20,30] Finally, we present the considerable challenges, solutions, and future scope, including benign green energy approaches, cost-effective materials, maximum output energy pulse, stability of charging/discharging, environmental concerns, and bio-degradable electrode materials, and exciting continuous innovation of high-performance LDH/CNT SCs.[11,12,31] Incredibly, these composites are likely to sustain a vital energy storage research arena for the research community for many years.[32–37]

## 2. Insight into supercapacitors and their storage mechanism

Supercapacitors or ultra-capacitors have attracted significant researcher interest as energy storage devices compared to other electrical passive components such as LIBs and capacitors due to their high power density, ultrafast charging/discharging rate, reasonable retention rate, long cyclability, and the ability to fill the gap between batteries and conventional capacitors. In general, SCs are classified as capacitors and complementary with rechargeable batteries in terms of energy density and power density because of their large specific surface area and short distance between the separator and electrodes as electron transport channels. Because the electrode–electrolyte boundary is limited without other reactions contributing to the storage mechanism, the charges from the electrolyte are attracted towards the electrodes upon the application of a potential to the cell[21,38] and interact at the surface of the electrode to form an electrostatic double layer (EDL),[12,30,39–43] contributing to the total specific capacitance with an equivalent series resistance (ESR). This EDL is responsible for all the properties of SCs, especially their energy density, which will eventually replace LIBs or capacitors if they demonstrate 100% energy capability. Meanwhile, their storage principle and mechanism take limitless advantage of putting other devices in the backdrop of the energy storage environmental setup, and the storage capacity depends on three essential components, *i.e.*, the electrode materials, electrolyte, and separator, as shown in Fig. 1(c). Regardless, the electrode and electrolyte solution interaction is vital to achieving a better specific capacitance, charge/delivery rate, stability, energy, and power density.[44]

### 2.1 Types of fundamental storage mechanisms in supercapacitors

The storage mechanism in SCs can broadly be divided into three types depending on the materials used as the electrodes, as illustrated in Fig. 1(d).

**2.1.1 Electric double layer capacitance mechanism (EDLC).** This mechanism is similar to that in conventional dielectric capacitors. The charge can be stored electrostatically at the interfacial area of the electrodes through reversible adsorption/desorption of ions at the boundary of the electrolyte and submerged stable electrochemically active electrode.[40] The capacitance obtained due to double-layer charged ion separation due to polarization occurs at the border of the electrode–electrolyte. A double layer is created because of the excess or lack of charges at the electrode surface, showing the development of opposite charges for neutrality. The effective capacitance increases due to the net charge stored directly at the double layer without crossing the interface, and the generation of charge combination takes place due to the adsorption/desorption ions from solution and defects in the crystal lattice in the electrode material.[12,18,45] This double layer thickness extends to a few nanometers and entirely depends on the electrolyte concentration, whereas it is independent of the ion concentration in the electrolyte, as shown in Fig. 2(a).

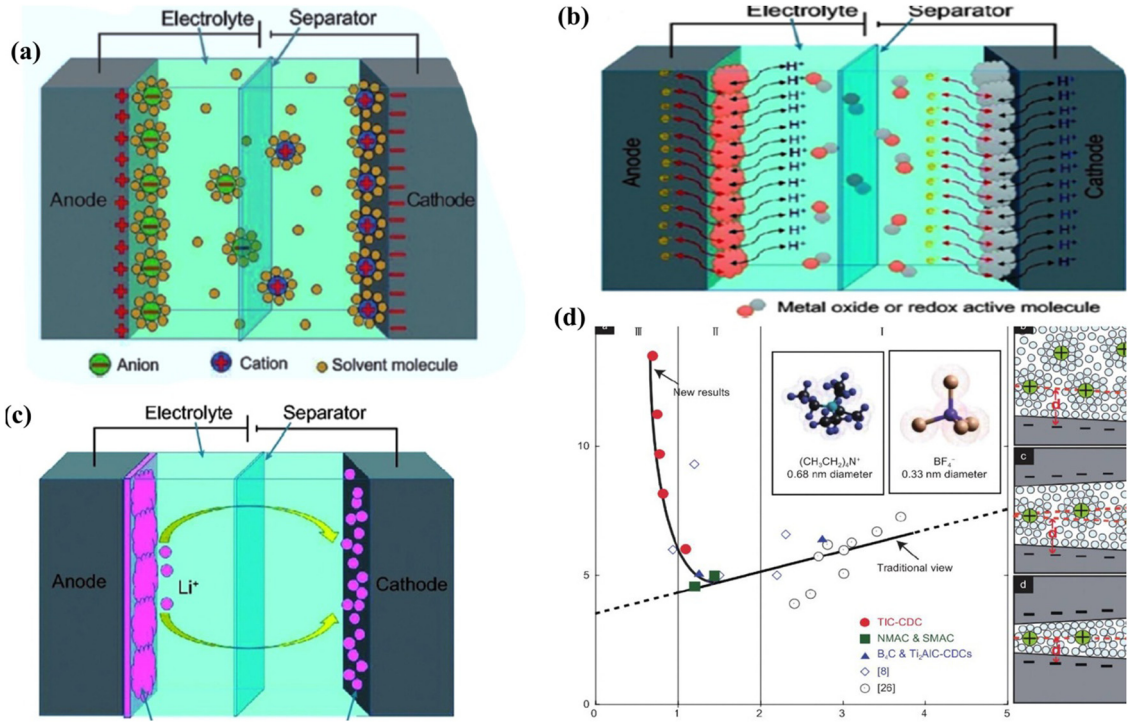


Fig. 2 Schematic of (a) an EDLC, (b) pseudocapacitor and (c) hybrid SCs. Reproduced with permission from ref. 16. (d) Graph of normalized capacitance *vs.* pore size in an electrolyte containing $TEABF_4$ dissolved in CAN and solvated ions in pores with different distant pore walls. Reproduced with permission from ref. 28.

The interfacial double charge mechanism was developed by Von Helmholtz in the early nineteenth century. According to theory, the opposite polarity charges form a double layer around the electrode, and the electrolyte maintains a distance equal to its atomic size and stores energy electrostatically. However, later, the Gouy–Chapman model assumed diffusion statistics at the double layer and followed the Maxwell–Boltzmann distribution law to calculate the capacitance, which is higher than that in the previous model given that the potential decreases from the interface. Combining the above-mentioned two models, Stern suggested that some ions, followed by Helmholtz's inner layer and outer compact layer, are called the Stern layer and diffusion layer, respectively. Again, the inner Helmholtz plane is very close to the electrode, and the outer Helmholtz plane is contacted with an aqueous electrolyte solution. The specific capacitance associated with EDLC can be calculated as follows:

$$C_s = \frac{AX\varepsilon_0}{d},$$

where '*A*' is the surface area of the electrode, '$\varepsilon_0$' is the permittivity of free space, and *d* is the Debye length, which is the width of the electric double layer.

The most popular EDLC materials are graphene, carbon nanotubes, and activated carbon given that they are cost-effective, are composed of different forms of carbonaceous materials, easy to synthesize, and their optimized pore size matches the electrolyte ion size. However, this technology has less energy density, *i.e.*, between 5 to 9 W h $kg^{-1}$. Thus, researchers are focused on the development of new electrolytes and modified electrodes to ensure better activity.

**2.1.2 Pseudocapacitors.** The energy storage in pseudocapacitors (PCs) is due to the redox reaction of the faradaic process, which provides a fast faradaic contribution to the capacitance. The demand for a high power density and a few seconds charging time drives the construction of new novel electrode materials.[46] The charge transfer occurs through the electrode and electrolyte oxidation and reduction process. Due to their redox activity, PCs are similar to batteries, but their energy storage type is electrochemically accompanied by the formation of a double-layer. Therefore, this type of capacitive electrode shows a higher energy density than EDLCs, as shown in Fig. 2(b). The nature of pseudocapacitance depends on the charge storage in the potential window. This is because the charge passes across the double layer with a capacitor value, according to the amount of charge applied and potential[9,12,14,40] as follows:

$$C = d(\Delta q)/d(\Delta V).$$

**2.1.3 Hybrid supercapacitors (HSs).** Hybrid supercapacitors were developed to increase the value of both energy and power density. This is because both values will always be addressed in the above-mentioned two mechanisms, where EDLC results in a high specific power, and PC delivers the maximum energy. Therefore, the hybrid SC concept emerged to combine one fundamental property with another, as shown in Fig. 2(c). Thus, it can be formed by coupling EDLC and

pseudocapacitive (PC) materials. The storage mechanism principle is generated by combining the principle of EDLC and PC. The charge stored by SCs depends upon certain factors, including specific capacitance, energy, power density, operating potential, and equivalent series resistance (ESR).[12,16,40]

### 2.2 Factors affecting the activities of supercapacitor

The working principle of SCs depends on many factors and variable parameters, resulting in milestone achievements in energy storage. For example, carbonaceous materials exhibit excellent activity due to their extraordinary properties, such as maximum surface area per unit mass, tunable crystal structure, ease and availability, and environmentally friendly nature.[47] These materials are obtained directly from nature or *via* synthesis methods such as carbonization and chemical or physical activation. Biomass or plant waste is the best example for extracting well-saturated porous carbon materials to enhance the electrode stability, specific capacitance, rate capability, energy density, and power density. These factors depend on some electrochemical components and the intrinsic properties of the electrode, which are briefly explained in Scheme 1.

(I) Electrode material: the electrodes are the heart in electrochemical cells, which are essential parts contributing to the performance of SCs.[6] Carbon-based composites provide an excellent opportunity to search for result-oriented supercapacitive values.[48,49] This is because they possess both physical and chemical activity at different kinetic temperatures and pressures. Meanwhile, carbon is the most suitable material for EDLC because of its various forms, such as nanotubes, nanofibres, nanorods, and quantum dots. The mobility of ions in carbon electrodes in the electrolyte enhance the EDLC property, which depends on the size of their pores. However, the electrostatic charge storage depends on the pore size of the electrode and its preference with the electrolyte ion size. This is why the specific surface area is considered to determine the pores in different forms of carbon.

(II) Specific surface area: the specific surface area based on the BET (Brunauer–Emmett–Teller) method is calculated using the adsorption/desorption isotherm in an $N_2$ environment. As a result, the higher surface area of the porous electrode will increase the specific capacitance.[8] However, the pore size should match the electrolytic ions for their absorption for charging/discharging, followed by the EDL process. There is an appropriate relationship between the specific surface area,[50] pore structure, and volumetric specific capacitance of the electrode. An increase in specific surface area leads to an

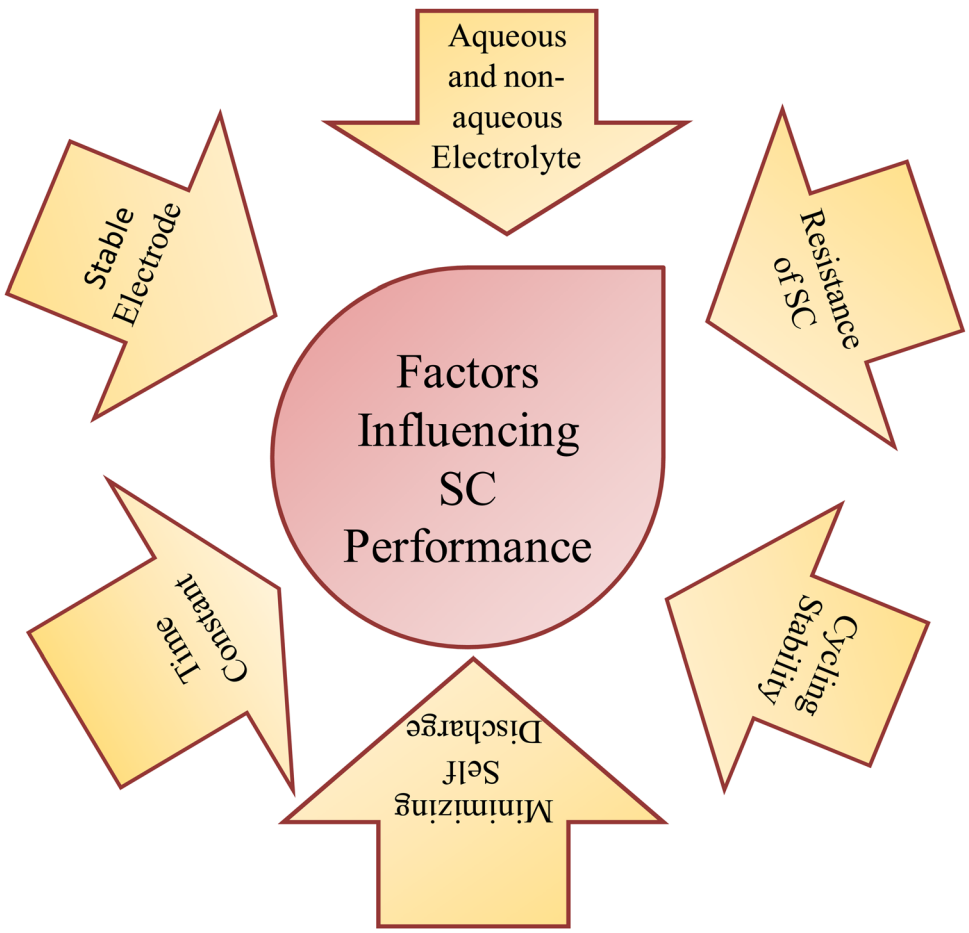


Scheme 1 Schematic summarizing the components contributing to the overall performance of hybrid SCs.

increase in pore structure but a decrease in density, resulting in a net reduction in volumetric specific capacitance. Thus, a must be achieved among pores, surface area,[3] and maximum specific capacitance for CNT/LDH composite electrodes. Meanwhile, there is a theoretical linear relationship between capacitance and area.

$$i.e.\ C = \frac{\varepsilon_r \varepsilon_0}{d} A, \quad (1)$$

where the symbols $\varepsilon_r$, $\varepsilon_0$, $A$ and $d$ represent the permittivity of free space (F $m^{-1}$), relative dielectric constant, surface area of the electrode ($m^2$), and dielectric between the ions in the electrolyte and the electrode surface, respectively.

(III) Morphology of electrode material: the leading performance of SCs depends on the morphology of the electrode material. This is because it provides the size and shape of nanoscopic and microscopic materials such as nanosheets, nanoparticles, and nanorods, which determines the arrangement of groups of molecules/atoms, not only to ensure their distribution pattern to form a pore structure but also information regarding the dimensions of LDH/CNT composites with absolute accuracy. Also, the pore size of the electrode should be greater than that of the electrolytic ions because of easy reversible faradaic electrocatalytic reaction.[50] The necessary synthesis is required to realize the appropriate morphology for combining electrodes to create easy and fast electron transport for generating more charge at the current collector, which enhances the capacitive value.

(IV) Pore structure: pore structure analysis is always challenging. It determines the pore size and shape,[28,51] and its distribution is always an impactful parameter for the specific capacitance and creating ion transportation channels *via* electrolytes and electrodes for storage devices. These ions must be associated with the size of pores because the size of pores should be much more than that of ions. The movement of ions in the electrolyte solution differs from their mobilization into pores. However, some articles indicate that smaller pore sizes (<1 nm) will result in greater energy values. Also, some reported a decrease in capacitance after diminishing the size of pores by two times, as shown in Fig. 2(d). Then $C_s$ will slightly increase on further reducing the pore size than solvated ions. Moreover, the prolonged building of pores on LDH/CNT asymmetric composites during the electrochemical reaction will enhance the fabricated electrochemical cell. Finally, $C_s$ will increase if the number of micro/nanopores increases. Thus, the number of pores and structures are responsible for the electrochemical activity.

(V) Nano-formulations: these are well-nano-structured materials suitable for ion transportation from the electrolyte to electrical storage systems *via* nanoporous electrodes.[41,52] They have a repeated, continuous order of lattices, and there is no structural defect, line defect, interstitial defect, or strain sustainability. Therefore, nano LDH/CNT composites affect the degree of crystallinity and for playing a tremendous role in the active electrochemical activity, leading to supercapacitors.

(VI) Mean free path: the average path traveled by ions is a crucial point in determining the charging/discharging rate.[41,45,49] The short displacement of ions in the electrolyte has the least interaction time with nano-porous LDH/CNT composites to convert chemical energy into electrical energy.[3] As a result, this advantage leads to supercapacitor characteristics of suitability, flexibility, and longevity on both the laboratory and commercial scales.

(VII) Choice of electrolyte: a suitable electrolyte will be inevitable to amplify the strength of SCs in terms of energy density, power density, specific capacitance, retention rate, cycle life, cycle efficiency, charge/discharge time, service life, zero self-discharge time, and preference over batteries and capacitors. The electrolytes are divided into solid and liquid states, popularly used as organic, aqueous, and ionic subtypes.[6] The significant properties considered are (i) high ionic conductivity,[40,44] (ii) good stability, (iii) wide voltage window, and (iv) maximum ion transport number.

(a) Organic electrolytes: these electrolytes have a broad potential window but low conductivity, and are more expensive. Therefore, they are unsuitable for commercial purposes. Another drawback of these electrolytes is their operating voltage of up to 3 V. Furthermore, they are flammable, hazardous, have a low boiling point[6] and low release of energy density. Also, their operation requires an inert atmosphere due to their volatility.

(b) Aqueous electrolytes: these electrolytes offer more advantages then organic electrolytes considering their properties such as non-flammability, high ionic conductivity,[40] low cost, and high rate capability, leading to a better capacitance and power density. Also, based on their pH value, they are classified into three types, including acid, base, and neutral electrolytes. This type of electrolyte is widely used because of its moderate potential window range, safety, low cost, stability, and abundant availability. However, their major drawback is the addition of antifreeze substances due to their freezing point approaching below zero degrees.[6]

(c) Ionic electrolytes: these ionic liquid-based electrolytes possess both organic and aqueous electrolyte characteristics with a potential range of up to 35 V. They show better conductivity, non-flammability, high thermal and chemical stability, low cost, and high rate capability, leading to a better capacitance and power density.[6]

Besides, polymer electrolytes are treated as the fourth most popular type due to their inherent properties such as conductivity, electrochemical stability, and corrosion resistance. However, they are not involved in side-reactions at the boundary between the electrolyte and electrodes.

## 3. LDH/CNT-based composites for supercapacitors

Presently, LDHs have emerged as unique materials to promote the charge capacity in a long-term process because transition-based material LDHs have distinct advantages over other

electrochemical energy storage materials, such as large specific area, tunable electric and thermal conductivity, and high mechanical strength. Also, they have differently tuned structural synthesis routes and chemical compositions at a low cost. Also, carbon nanotubes (CNTs) are the most impressive, reliable, and excellent potential cylindrical materials with high electrical conductivity,[46] mechanical stability, high corrosion resistance, and large surface area, making them ideal candidates for charge conduction.

### 3.1 Advantages of LDH/CNT composites

Layered double hydroxides and carbon nanotubes have received remarkable attention due to their extensive properties for advanced asymmetric energy storage electrodes. Herein, an electrostatic assembly of LDH/CNT resulted in an improvement in electrical conductivity, mechanical strength, and chemical reactivity, facilitation of electron transfer, specific capacitance, and subsequently massive electrochemical application. Typically, these composite materials are promising material for electrochemical tests due to their good functionality, long cycle consistency, high velocity capability, and appropriate interlayer spacing for ions, which is helpful for reversible transfer and the storage of maximum ions. Some of the features are listed pictorially in Scheme 2.

• LDHs composited with carbon materials show improved conductivity, high specific capacitance, larger integral area, good rate performance at low current density, flexible ion exchangeability, high crystallinity, stability, increased number of active sites and improved energy storage efficiency. Besides, these compounds are eco-friendly and sustainable combinations with excellent electronic properties, leading to new composite materials and attracting new technological interest in recent years.[53] Their advantages are high electroactivity, maximum exposure of active sites, enhanced conductivity, and reduced volume change during the charge/discharge process.

• Also, composites (LDH/CNT) grown without adhesion show improved conductivity,[44] reduced interface resistance, increased contact area between the active substances and electrolyte, shorter diffusion distance, improved electron transmission efficiency, and then boosted redox reactions at the boundary between the electrode and electrolyte.

Another advantage is that the resistance of these composites can be significantly reduced by forming a 3D nano-core–shell structure, which leads to electrochemical stability and high rate capability.[54,55]

• The multilayer structures of LDH/CNT nanocomposites consistently achieve excellent electrical conductivity, extraordinary cycle performance, and pseudo-capacitance, which are further enhanced by coupling with different nano-structured carbon species in an effective systematic investigation.[56]

• If the slash in the EIS plot is nearly 90°, it indicates pure capacitive behavior, greater energy density, and low diffusion resistance of ions in the nanocomposite structure, which determines the conductivity, signifying the importance of hybrid composites.[42,57] Therefore, with the optimal composition, these composite structure LDH/CNT electrodes show a worthy performance. It is necessary for redox reactions to improve their electrochemical behavior and resolve the conflict between mass loading and electrochemical performance.

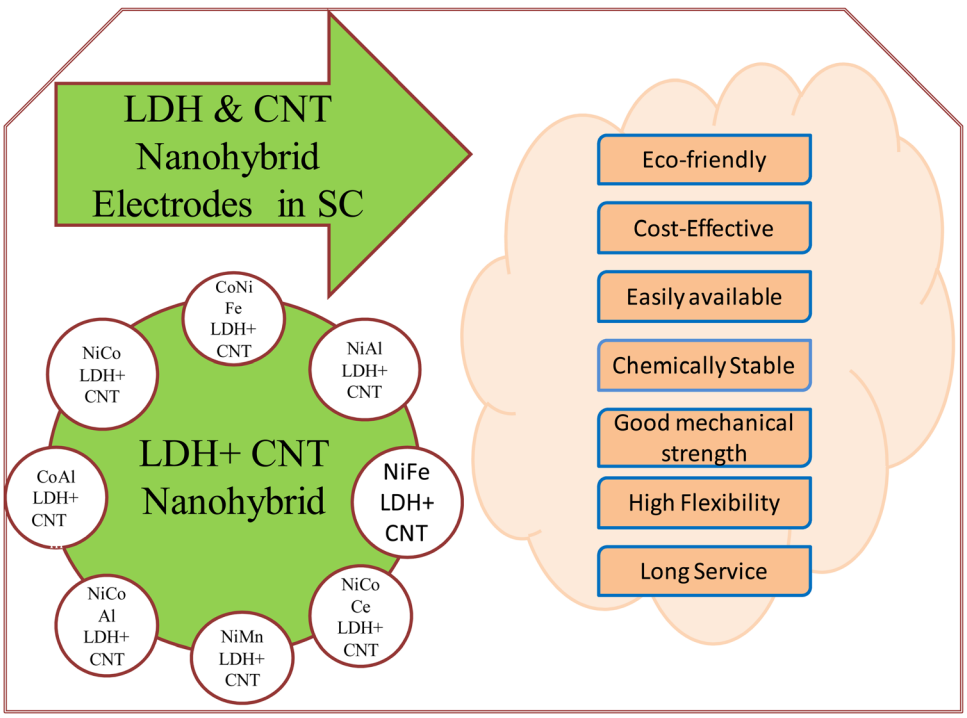


Scheme 2 Presentation of novelty, advantages, and human-friendly LDH/CNT nanohybrids.

Table 1 List of different LDH/CNT composite electrodes for SC application

| S. no. | Layered double hydroxides | Merit points | Ref. |
|---|---|---|---|
| 1 | CoAl LDH | Improved electrode stability and fast ion transport | 2 |
| 2 | NiCo LDH | Better safety, low price, and maximum specific capacitance | 58–61 |
| 3 | CoNiFe LDH | High surface area, remarkable electrochemical performance, and better energy and power density | 62 and 63 |
| 4 | NiAl LDH | Synergistic effect of both CNT and LDH, wide potential window, high specific capacitance | 64 and 65 |
| 5 | NiFe LDH | Wide potential range, better cycling stability, and excellent energy and power density. | 66 |
| 6 | NiGa LDH | Tunable crystal structure, apparent morphology, and specific area. | 67 |
| 7 | NiMn LDH | High specific capacitance, long life span, and stability | 68 |
| 8 | NiV LDH | Facilitate electron transport & improving cycle stability | 69 |
| 9 | NiCoCe LDH | Marvellous retention rate, appropriate surface area, and excellent electron conductivity. | 7 |
| 10 | NiCoAl LDH | Maximum pseudocapacitive electrode material | 70 |

### 3.2 LDH/CNT-based symmetric/asymmetric supercapacitors

Different types of electrodes have been employed to study their properties, morphology, and applications, listed in Table 1.

**3.2.1 CoAl LDH.** A noteworthy CoAl LDH/CNT structure is one of the excellent examples of an electrode material used for its electrochemical performance based on its improved conductivity, chemical stability during prolonged faradaic reaction, high surface area for increase in the number of active sites, *in situ* growth beyond adhesives, and enhanced kinetics of electron transmission in the electrolyte. This is because multiwall CNTs with LDHs will show improved electrode stability and enhanced ion transport facility. Therefore, CNT/CNH carbon materials formulated with CoAl LDH@CNT/CNH produced a synergistic effect in specific capacitance than the pristine LDH.[2]

**3.2.2 NiCo LDH.** The innovative, remarkable hybrid structure of NiCo LDH/CNT supports outstanding energy generation achievements and storage for all-solid-state asymmetric SCs.[58] This composite supports stable structure, electrochemical stabilization, high surface area, prevention of LDH stacking, and conductivity, which enhanced the electrochemical performance of MX–CNT–LDH when nitrogen was doped on carbon-coated CNT as a 3D core–shell structure.[59] Also, both LDH and MXene in the composite promote the conductivity and capacity, which strengthens the pseudocapacitive materials.

Again, CNT/NiCo LDH nanohybrids shorten the electron and ion pathway and prevents the agglomeration of LDH when MOF-derived CNT is further developed with *in situ* synthesized carbon fibers. Therefore, it possessed an improved chemical structure and active sites. Also, 3D CNT networks possess a large, accessible and conductive area with LDH to produce high electrical conductivity, enabling fast electron transfer in electrolytic cells, marvelous specific capacitance with better retention, and controlled charge–discharge stability.[60] Moreover, 3D-structured CNT@CoS-anchored LDH enhanced the conductivity of the electrodes and structural stability and electrochemical performance due to the synergistic effect of cobalt sulfide and hydroxide.

In addition to ternary electrode systems, the NiCo LDH@$Co_3S_4$/CNT nanocomposite showed an impressive capacity and high rate capability and conductivity compared to individual electrodes, indicating its practical usage in hybrid SCs in energy storage devices due to its core–shell structure, leading to good contact sites and synergistic effect. Alternatively, LDH/CNT pseudo-capacitor electrodes are considered advanced energy storage devices because of their outstanding records regarding specific capacitance, energy density, and surface area when lamellar hierarchical LDH nano cables are prepared on conducting CNT networks. However, it is interesting to find superior SC performances when the composite LDH/CNT/NF acted as the positive electrode and AC (activated carbon)-based carbon as the negative electrode, exhibiting better cell capacitances and electrochemical performances for high energy and power density asymmetric SCs.[61]

**3.2.3 CoNiFe LDH.** A novel ternary CoNiFe LDH was intercalated with SDS (sodium dodecyl sulphate) and CNT to improve its layer spacing and charge transfer and form a porous flower-like structure to generate more active sites, high specific capacitance, and retention rate because of the intercalation of anions, which increased the layer spacing and high charge transfer rate. Moreover, the addition of CNT or carbonaceous materials reduces the charge transfer resistance. This confirms the strategic compound formation for the successful fabrication of portable, environmentally friendly, cost-effective, and all-supported high-performance wearable SCs.[62]

Although trimetallic CoNiFe LDH showed restricted electrical conductivity, its composite with CNT is a mature electrode that facilitates the transfer of ions and electrons and supports high active sites, large surface area, structural tunability, and electrochemical performance. Especially, the hybrid asymmetric composite enhanced the energy and power density, long cycle life, maximum retention rate, and better capacitance capability. Fe is used for boosting the electrochemical reaction, which is better than pristine LDH.[63] Thus, the output of CoNiFe LDH/CNT as a promising electrode material suggests the optimization of the electrochemical data for the fabrication of perfect hybrid SCs.

**3.2.4 NiAl LDH.** NiAl LDH is a unique layered structured pseudocapacitive material that always favors reversible faradaic reaction, performing the best in electrochemical activity in combination with carbon materials. However, the key factor of LDH in energy storage devices is to fabricate only well-defined nanostructures, and thus the material will enhance the electrical conductivity of symmetric/asymmetric electrodes. Also, it is one of the most preferable composites because of its

easy preparation and stable structure. Although pure LDH shows some limitations in terms of electrochemical performance, conductivity, ion/electron transfer, capacitance, *etc.*, these issues can be solved by intercalating CNT or graphene and optimizing the parameters. Given that CNTs support oxides/hydroxides, eliminating the restacking issues in LDHs improves their chemical stability, speeds up the faradaic redox reaction, and leads to an emerging material for EES and conversion devices.[64]

A novel ternary composite cellulose-based CNT/cellulose//NiAl LDH was formed to study its electrochemical performance with a variation in the CNT/cellulose composition ratio and enable the fabrication of a flexible SC, where cellulose was extracted from various waste sources, including grass, tissue paper, and rice straw, and modified with CNTs. The specific capacitance, impressive energy density, cycle stability, retention rate, and Ragone plot confirmed the experiment with a blue LED bulb, which glowed intensely, creating a cheaper, more efficient, and portable future electronic device.[65] Together with the diverse potential of CNTs, the synergistic effect of LDH composites has been observed, making them leading candidates in the storage field due to their greater number of active sites, long cycle life, and recorded cycling stability. Alternatively, NiAl LDH embedded into 3D interconnected CNTs produces abundant redox active sites and sufficient room for buffer expansion to enable fast electron transfer, and consequently high electrical conductivity.

Thus far, these composites have shown the maximum specific capacitance and good cycle stability due to their long-range connection to avoid electron transport disruption. Given that CNTs act as a conductive path due to their interfacial contact with LDH lamellar nanosheets, cell reactions can proceed to realize charge storage at both sides of the current collector. In the case, of the ternary nanocomposite mesoporous hybrid NiAl LDH/CNT/GNS (graphene oxide sheets), it exhibited a high specific capacitance, long cycle-life, and fantastic cycle stability due to both its carbonaceous CNT materials and GNS support as a conductive substrate, as well as free-electron transmission route in the LDH interlayer.[57]

**3.2.5 NiFe LDH.** NiFe LDHs are valued candidates to form composites with CNT, rGO, and FeO at a particular temperature given that the NiFe LDH–CNT–rGO–FeO electrode prevented the stacking of layered structures and promoted quick electron/ion transmission for energy storage and more conducting channels. Also, sometimes NiFe LDH/rGO/CNF (carbon nanofibers) can act as an excellent three-electrode system for SCs rather than the LDH/CNT asymmetric composite in terms of capacitance, energy density, and cycle stability due to extensive surface modification of CNF, and therefore the enhancement in conductivity, specific surface area per unit mass and porosity, fast electron/ion transfer, and stable and tunable structure for the fabrication of EES devices.[66]

**3.2.6 NiGa LDH.** Owing to the unique structural design of NiGa LDH with porous CNTs derived from an MOF, it was used as an excellent conductive skeleton for the reduction of the electron diffusion path, stopping agglomeration, reduced volume expansion due to excessive charges and discharges, and breakthrough electrochemical performances for asymmetric SCs having high cycle stability and retention rate.[67]

**3.2.7 NiMn LDH.** Despite the large usage of LIBs and electrochemical capacitors for typical energy storage and conversion, NiMn-based LDH and CNT composites or other electrodes lag behind LIBs because of some limitations in high electric power sources. However, NiMn LDH has attracted significant attention due to its power density, long life span, capacitance retention rate, and physicochemical and electrochemical properties. Furthermore, this type of LDH ensures sufficient pseudocapacitance behavior due to its large surface area, and CNT serves as the backbone for synergistic conduction to facilitate electron transport channels, provides large space for volume expansion in the active sites, and promotes exceptional electrochemical measurement for light-weight storage equipment.[68]

**3.2.8 NiV LDH.** Given that the vanadium element supports multiple oxidation states, has high abundance, and high power density, it has been suggested as one of most suitable SC electrode materials with CNT as NiV LDH composites to realize excellent electrochemical evaluation. This reveals the extraordinary outputs of SC applications, implying their great potential for energy storage.[69]

**3.2.9 NiCoCe LDH.** Cerium ($Ce^{3+}/Ce^{4+}$) doping improves the conductivity and active site density, which tends to increase the surface area, rate properties, long cycle stability, specific capacitance, and all the electrochemical properties in NiCoCe LDH/CNT nanocomposites in comparison to LDH/CNT without Ce.[7] Hence, this asymmetric hybrid SC electrode shows potential for further study and optimization of the energy storage and conversion field parameters.

**3.2.10 NiCoAl LDH.** Nano-structured carbon composites such as CNTs have always served as pillars of strength in the electrochemical performance of ternary NiCoAl LDH–CNT/rGO nanostructured pseudocapacitive hybrid electrode composite materials, which can be used in various energy storage devices because of breakthrough answers in capacitive performance, power density, and cycling stability.[70]

# 4. Synthesis and physico-chemical characterization of LDH/CNT-based hybrid composites

The different synthesis and characterization methods for LDH/CNT flexible composite electrodes are discussed.

## 4.1 Synthesis methods

Different synthesis methods are adopted to prepare composites from different alkali or transition metals with additives to form a strong, suitable, sustainable, harmless, and eco-environment rigid electrodes to produce the desired outcomes. These methods include hydrothermal, solvothermal, co-precipitation, thermal deposition, and chemical deposition. They are the most convenient, suitable, easy, and cost-effective methods

Table 2 Classification of various synthesis techniques with their advantages and disadvantages

| S. no. | Synthesis technique | Advantages | Disadvantages |
|---|---|---|---|
| 1 | Hydrothermal | Efficient, economical, best purity sample and good crystallinity. | The equipment costs a little amount & long period results in higher energy use. |
| 2 | Solvothermal | Minimal loss of nanomaterials, good crystal growth, and improves structural defect. | Costly equipment and the necessity of high-temperature |
| 3 | Coprecipitation | Simple, pure, and homogeneous material preparation technique | The final product contains the solution of salt, while separation occurs |
| 4 | Electrodeposition | Increases conductivity and durability. | High cost, limited thickness, and sensitivity to electrode structure. |
| 5 | Reflux | Speeds up the reaction; no loss of solvent may evaporate reaction byproducts. | Superheating and cooling take too much time. |
| 6 | Chemical deposition | Uniform thickness, conducting films, high purity and controllable. | High-temperature requirement, high throwing power. |
| 7 | Thermal chemical vapor deposition (TCVD) | Selectively more accessible method, material deposited on specific regions. High purity and easy control | Stress formation and high diffusion rate |

for achieving high yield, producing a compound with a porous structure free from contamination and moisture and without releasing harmful gases into the atmosphere. In terms of effectiveness, these techniques can methodically guide researchers under various circumstances and with different parameters. Every synthesis method has advantages and drawbacks, as listed in Table 2.

(I) Hydrothermal

The hydrothermal is a low-cost, simple, and aqueous solution used as a sample preparation technique. The material is placed in a high-temperature-pressure built muffle furnace in a closed Teflon-lined vessel for a stipulated time. It is the most facile process, especially and particularly for the synthesis of nanoparticles and their appropriate composites for application under ambient conditions in energy storage and electricity generation.[71] This is the most common eco-friendly solid-state synthesis method for the preparation of LDH, which forms a good-quality crystalline phase with specific properties and controllable composition, together with control of the temperature, producing high yield, homogeneously synthesized, pure, novel nanomaterials. On average, hydrothermal synthesis is a powerful tool for developing advanced materials with tailored properties.

To improve the activity of CoAl LDH-based electrode materials for energy storage applications, Zhang *et al.* modified the CoAl LDH electrode material by adopting a one-step hydrothermal method to synthesize CoAl LDH/carbon-based composite integrated electrode materials including CoAl LDH/CNT, CoAl LDH/g-$C_3N_4$ and CoAl LDH/AC.[2] In a typical synthesis method, $CoCl_2{\cdot}6H_2O$, $AlCl_3{\cdot}6H_2O$, $NH_4F$, and urea were employed as the precursor materials in three separate beakers. Then, g-$C_3N_4$, CNT, and AC (activated carbon) were added to the beaker separately. Then, 75 mL DI water was added to the above solution and stirred for 30 min, together with pretreated nickel foam, and subsequently subjected to hydrothermal treatment at 115 °C for 14 h to obtain Ni foam-deposited CoAl LDH/g-$C_3N_4$, CoAl LDH/CNT, and CoAl LDH/AC, respectively. Moreover, the authors varied the solvent composition to study its effect on the electrochemical performance of the CoAl LDH composites. Also, the authors found that by adopting this type of hydrothermal method, the electrode material can be *in situ* grown on Ni foam without using adhesives, which results in improved conductivity, reduction in interface resistance, increase in the contact area between the electrode and electrolyte, enhanced electron transmission efficiency, and enhancement in the overall electrochemical performance.

The conductive modification of CoAl LDH by conductive additives such as super P, rGO, carbon nanotubes (CNT), and carbon nanohorns (CNH) was reported by Yang *et al.*[72] to investigate its electrochemical performances. However, only the binary conductive additive of CNHs/CNTs in the form of CoAl LDH@CNT/CNHs provided significant results because of the efficient long-range electron transmission. The first step involved the preparation of CNH *via* DC arc discharging in liquid $N_2$ between two graphite electrodes with different diameters, whereas rGO, CNTs, and super P were directly purchased. Alternatively, a slurry of the synthesized LDH (85 wt%), required amount of PTFE (5 wt%), and respective proportion of conductive additives (10 wt%) (super P, CNHs, CNTs, rGO, SP + rGO, SP + CNT, SP + CNH, rGO + CNT, rGO + CNH, rGO + SP, and CNT + CNH) was homogeneously mixed by adding DI water, followed by persistent magnetic stirring for a few hours. Finally, this composite slurry was coated uniformly on Ni foam for 12 h at 70 °C to obtain the CoAl LDH@CNT/CNH hybrid electrode. Herein, the construction of binary conductive additives contributes to the synergistic effects on conductivity.

Again, Yu *et al.*[73] presented a novel composite of exfoliated positively charged CoAl LDH nanosheets and negatively charged carbon nanotubes fabricated *via* electrostatic attraction. Initially, cobalt chloride, aluminium chloride, and urea were dissolved in DI water and stirred for 2 h at room temperature, which was further autoclaved at 120 °C for 8 h. Then, a pink precipitate of LDH was centrifuged and washed with DI water and ethanol to obtain a mixture of carbonated, exfoliated and unexfoliated LDH. Now, the carbonation of LDH was removed by adding it to $NH_4Cl$, $NH_4NO_3$, $NaNO_3$, and 25 wt% aqueous solution of tetramethylammonium hydroxide, transferred to shake for 12 h. Meanwhile, the unexfoliated CoAl LDH could be removed by dispersing it in formamide, followed by shaking it at 160 rpm for 2 d. Now, the conductive additive CNTs were modified by ultrasonication for 30 min, and

subsequently refluxed in 9 M $HNO_3$ at 100 °C for 12 h. Then, the mixture was vacuum filtered, washed, and dried, and the oxidized CNTs were poured into 4 M NaOH aqueous solution under $N_2$ at 80 °C for 8 h. Now, this slurry was filtered, washed, and dried at 60 °C for 24 h and adjusted to neutral after treatment with an aqueous solution of NaOH. Finally, CoAl LDH nanosheets and modified CNTs were intercalated by adding the required amount of both to formamide, which was subjected to shaking at 160 rpm for 2 d to prepare the CoAl LDH–CNT composite with chemical stability and enhanced electrochemical performance.

A 3D core–shell structure of N-doped CNT/CoNi LDH was developed *via in situ* growth by Liu *et al.* for the fabrication of solid-state asymmetric SCs, as shown in Fig. 3(a).[58] In general, this research group tried to prepare N-doped CNT by heating polyaniline-coated CNT composites at 800 °C for 2 h in the presence of $N_2$. Then, CoNi LDH embedded on N-CNT from the raw materials of nickel nitrate, cobalt nitrate, and methenamine were added to the N-CNT dispersion in 1 : 1 ethanol and DI water and sonicated for 20 min. After that, the resultant was heated at 80 °C for 8 h, followed by filtration and freeze-drying to obtain the N-CNT@CoxNi LDH pristine capacitive electrode, which possessed a high specific surface area, stable structure, excellent specific capacitance, and good electrochemical stabilization. Again, another self-sustaining electrode, CoNi LDH, was built on a substrate of MXene and MWCNT by Ma *et al.* following a one-step hydrothermal process. In the first approach, MXene few-layer nanosheets were prepared using a certain amount of LiF dispersion in HCl solution, as shown in Fig. 3(b).[59] Then, $Ti_3AlC_2$ was slowly added and stirred at 40 °C for 48 h. Subsequently, the product was washed, centrifuged, and ultrasonicated to convert it from multilayer to few-layer MXene. Then, further nanosheets could be recovered after freeze-drying. Alternatively, in the case of the MXene–CNT–LDH composite, a homogeneous mixture of a few layers of MXene and MWCNT was dissolved in DI water and ethylene glycol, which was further stirred *via* ultrasonication and named solution 'A.' Now, $Co(NO_3)_2{\cdot}6H_2O$, $Ni(NO_3)_2{\cdot}6H_2O$, and hexamethylenetetramine were added to the above-mentioned solution with continuous stirring as solution 'B.' Solution 'B' and cleaned NF were subjected to hydrothermal treatment at 180 °C, followed by washing and drying to get highly conducting, excellent electrochemical stability, and high energy density, furnishing promising electrodes.

Another study was reported by Ding *et al.*[62] about the intercalation of sodium dodecyl sulfate (SDS) with hierarchical CoNiFe LDH with different carbonaceous materials including carbon black (CB), carbon nanotubes (CNTs), and carbon nanofibers (CNFs), which were denoted as CoNiFe (SDS) LDH/CB, CoNiFe (SDS) LDH/CNT, and CoNiFe (SDS) LDH/CNF, respectively. In the first step, CNTs and CNFs were functionalized by ultrasonic dispersion in $HNO_3$ and refluxed at 100 °C for 12 h, as shown in Fig. 4(a). The novel composites were fabricated using the precursors of $NiCl_2{\cdot}6H_2O$, $FeCl_3{\cdot}9H_2O$, $CoCl_2{\cdot}6H_2O$, CB (CNT & CNF), and $NH_4F$ dissolved in ultrapure water. The mixture was heated immediately at 160 °C for 12 h after adding SDS to obtain a CoNiFe (SDS) LDH/CB highly stable effective electrode for asymmetric SCs in a one-step hydrothermal process. Similarly, CoNiFe (SDS) LDH/CNT and CoNiFe (SDS) LDH/CNF were manufactured

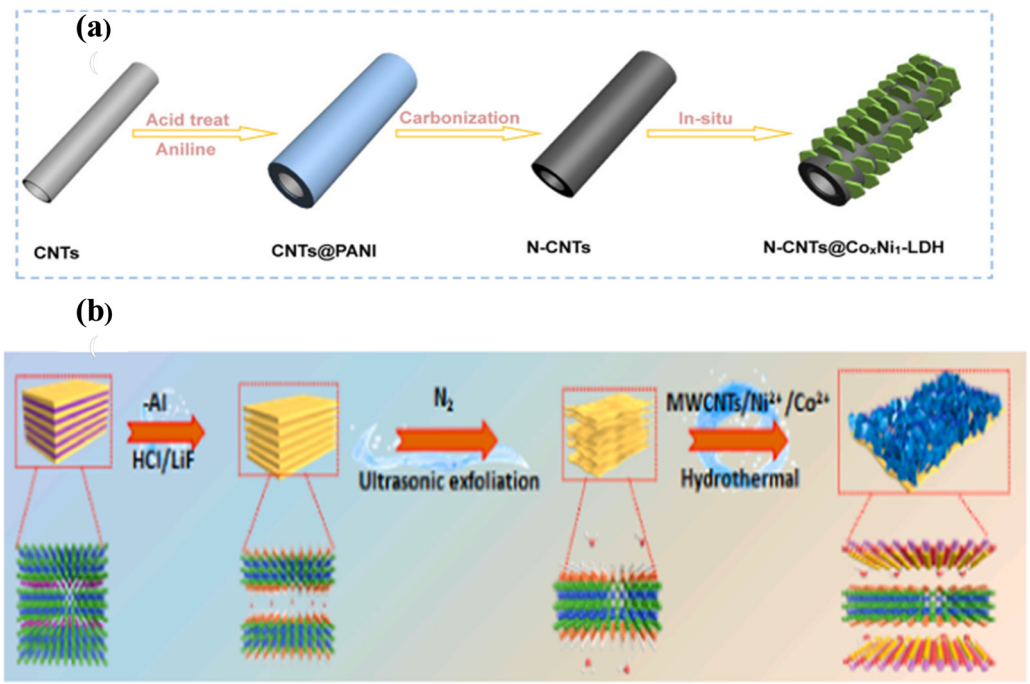


Fig. 3 (a) Process for the preparation of N-CNT@CoxNi LDH. Reprinted with permission from ref. 58. (b) Schematic of the synthesis of MXenes–CNT–LDH. Reproduced with permission from ref. 59.

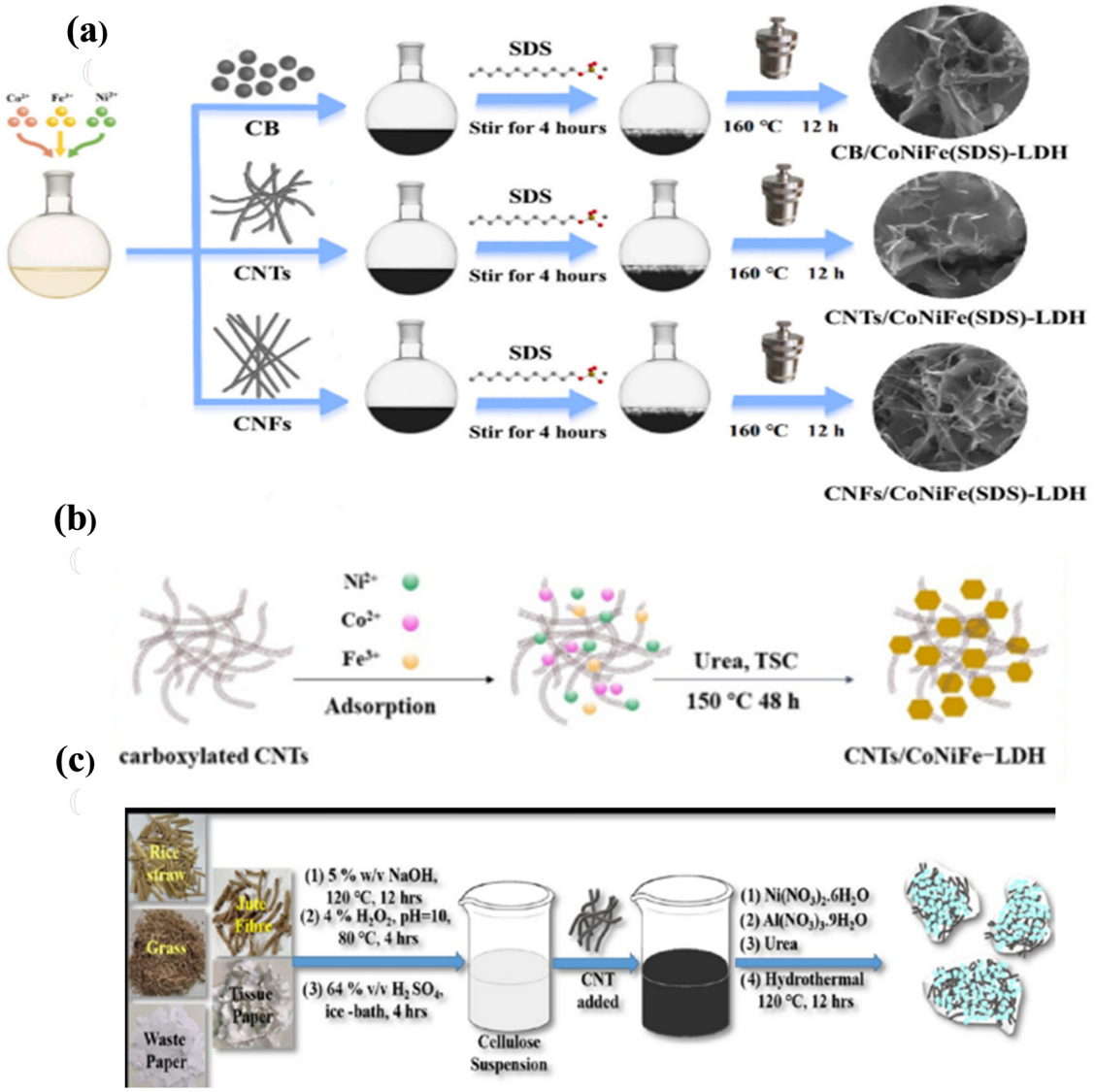


Fig. 4 (a) Schematic representation of the synthesis of the CoNiFe (SDS) LDH/CNT composite. Reproduced with permission from ref. 62. (b) Representation of the process for the synthesis of CoNiFe LDH/CNT. Reproduced with permission from ref. 63. (c) Schematic of the NiAl LDH/CNT cathodic composite. Reproduced with permission from ref. 65.

with the addition of CNT and CNF, respectively, in varying concentrations of SDS.

Moreover, a self-supported nanocomposite ternary LDH/CNT (CoNiFe LDH/CNT) electrode was first prepared by Wang *et al.*[63] *via* a one-step hydrothermal process, which possessed a high specific surface area, enhanced electrochemical performance, and outstanding conductivity for asymmetric SC. The steps involved in the preparation of carboxylated CNT from pristine CNT were dispersion in concentrated $HNO_3$ under ultrasonication and refluxing at 100 °C for 12 h. The next step was the preparation of the LDH/CNT integrated composite from the raw materials of $CoCl_2{\cdot}6H_2O$, $NiCl_2{\cdot}6H_2O$, $FeCl_3{\cdot}6H_2O$, $C_6H_5Na_3O_7$, and urea dissolved in a carboxylated CNT dispersion. Then, the mixture was subjected to hydrothermal treatment at 150 °C for 48 h, followed by rinsing and drying at 80 °C as a low-cost, eco-friendly, easy process to obtain the high mechanical strength CoNiFe LDH/CNT hybrid electrode, as shown in Fig. 4(b).

Again, another fabulous article about the extraction of nanocellulose from waste material combined with CNT and NiAl LDH was reported by Acharya *et al.*,[65] showing that cellulose–CNT–LDH is a cheaper cathode with high energy and power density for application in commercial SC devices. The first step involved the extraction of nanocellulose from different waste materials. Secondly, $Ni(NO_3)_2{\cdot}6H_2O$, $Al(NO_3)_2{\cdot}9H_2O$, and urea were dissolved in DI water, stirred and subjected to treatment in an autoclave vessel at 120 °C for 12 h, followed by rinsing with water and ethanol and drying to procure a new pseudocapacitive NiAl LDH, shown in Fig. 4(c). Here, for the fabrication of nanocellulose CNT–LDH composites, $Ni(NO_3)_2{\cdot}6H_2O$, $Al(NO_3)_2{\cdot}9H_2O$, and urea were employed as the precursors and to a homogeneous mixture of a fixed ratio

of cellulose : CNT in water. Then, the solution was subjected to hydrothermal treatment at 120 °C for 12 h. The product was rinsed with water and alcohol several times to obtain a neutral biomass-derived composite as an effective SC electrode for renewable and sustainable energy applications.

An NiAl LDH/CNT nanocomposite was prepared by Bai *et al.*[74] *via* a facile one-step precipitation process. This procedure involved the conversion of pristine CNT to acid-treated CNT under reflux at 100 °C for 12 h. Then, nickel nitrate, aluminum nitrate, and urea were added to the suspension of CNT in DI water with constant stirring and subjected to hydrothermal at 100 °C for 24 h, followed by filtration and vacuum drying to acquire resultant formulations, achieving and excellent specific capacitance, long cycle life and good capacitance retention rate.

In the study reported by Wang *et al.*,[64] they supported the growth of NiAl LDH nanoflakes on CNT *via* the hydrothermal approach to form a 3D core–shell structure. $SiO_2$ and AlOOH were employed to functionalize the CNTs to form a CNT/$SiO_2$/AlOOH (CSA) composite. In a typical process, CNT and CTAB (cetyltrimethylammonium bromide) were added to an aqueous solution of $H_2O$ and ethanol under continuous stirring. Then, NaOH and TEOS (tetraethyl orthosilicate) were added dropwise with vigorous stirring to form a black precipitate and filtered, rinsed, and dehydrated to get silica-modified CNT. Subsequently, the $SiO_2$-modified CNT was dispersed in AlOOH solution for 3 h. Finally, the product was centrifuged and washed with DI water and ethanol to obtain the CNT/$SiO_2$/AlOOH composite. In addition, a small quantity of $Ni(NO_3)_2$ aqueous solution was added dropwise into a dispersion of the CSA composite in DI water with constant stirring. Then, the mixture was transferred to an autoclave and heated at 100 °C for 6 h, subjected to centrifugation, followed by rinsing with DI water and ethanol several times for the arrangement of LDH on the CNT surface to obtain NiAl LDH/CNT for potential application in energy storage devices.

A novel NiFe LDH composite with carbonaceous materials was intensely studied by Wang *et al.*[75] for asymmetric supercapacitors, showing great potential for commercial energy storage applications. They constructed NiFe LDH/CNF, NiFe LDH/CNT, NiFe LDH/rGO, and NiFe LDH/rGO/CNF *via* a single-step hydrothermal approach and studied their electrochemical properties in three- and two-electrode systems. The authors assumed the *in situ* growth of the LDH composite considering the addition of $Ni(NO_3)_2{\cdot}6H_2O$, $Fe(NO_3)_3{\cdot}9H_2O$ to DI water containing CNF, CNT, and GO under ultrasonication with different mass ratios of GO and CNF mixture forming a homogeneous slurry. Then, the above-mentioned mixture was subjected to hydrothermal reaction at 150 °C for 48 h. The final pure carbon composites were collected after vacuum filtration, washed with DI water and alcohol, and dried overnight.

Again, Dinari *et al.*[7] reported the preparation of Ce-doped NiCo LDH/CNT nanocomposite electrodes to obtain the best electrochemical properties for energy conversion and storage applications for high-performance SCs. Firstly, cobalt nitrate nonahydrate, cerium nitrate hexahydrate, nickel nitrate, and ammonium fluoride were added to CNTs and dispersed in ultra-pure water under stirring for 30 min. Then, another solution of NaOH and $K_2CO_3$ was added dropwise to the above-mentioned mixture and stirred for 6 h. Ultimately, Ce–NiCo–LDH/CNT was obtained after centrifugation, washing with DI water and ethanol, and vacuum drying.

An MOF-derived LDH composite was designed by Huang *et al.*[60] to realize competitively enhanced energy and power density, electrochemical stability, and crystallinity for hybrid SC devices. In the first step, a solution of $Co(NO_3)_2{\cdot}6H_2O$ and $NiCl_2{\cdot}6H_2O$ in DMF was added dropwise to a solution of CNTs in DMF containing PTA under stirring and subjected to treatment in an autoclave at 120 °C for 16 h. Then, the product was rinsed with ethanol and dried to obtain CNT/NiCo MOF. Alternatively, NiCo LDH/CNT developed from CNT/NiCo MOF was dispersed in KOH solution under stirring for 5 h, followed by centrifugation, washing in DI water and ethanol, and drying at 60 °C.

(II) Coprecipitation process

This method is unique, eco-friendly, cost-effective, and convenient for investigating nanomaterials. Also, it is a subclass of the precipitation method, which is carried out when the precipitates of a soluble substance are formed under specific conditions. Generally, in a colloidal suspension, when substances reach supersaturation, nucleation takes place and growth occurs *via* the diffusion of suspended nanoparticles. The size, crystal structure, and morphology[76] of NPs can be controlled by slowing down the nucleation, ion concentration, and pH of the solution during growth. The fundamental characteristics are as follows:

- Nucleation plays the leading role for control the size.
- The products are insoluble species.
- The other factors affecting the size, morphology, and properties[77] are aggregation and Ostwald ripening.

Overall, this cost-effective process leads to the formation of scalable homogeneous mixtures with controlled compositions and particle sizes to produce nanoparticles, which are crucial for consistent performances in applications.

Employing the coprecipitation method, the unique synthesis of NiAl LDH/CNT was performed by Luo *et al.*[78] for the large-scale and environmentally friendly preparation of electrode materials for high-performance SCs. Meanwhile, the precursor mixtures of $Ni(NO_3)_2{\cdot}6H_2O$ and $Al(NO_3)_3{\cdot}9H_2O$ in DI water were mixed in a complete dispersion medium of carboxyl CNT in DI water under stirring. Then, an alkaline solution of $Na_2CO_3$ and NaOH was added dropwise into the above-mentioned solution and stirred continuously until the pH reached 10.5. Then, the solution was heated at 60 °C for 12 h, and filtration, rinsing, and drying were performed to collect the proposed NiAl LDH/CNT composite, exhibited a synergistic effect towards high-performance energy conversion and storage devices.

In an attempt by Yue *et al.*,[79] they expressed their view on synthesizing NiCo-layered double hydroxide and CNT@CoS hollow nanocages to produce better SC activity. Initially, the CNT/CoS precursor was derived when a small amount of carboxylated MWCNT and $Co(NO_3)_2{\cdot}6H_2O$ were added to

methanol with stirring, followed by the addition of 2-methylimidazole to the solution to construct CNT/ZIF-67. Then, the precursor was formed after the formation of a solid precipitate with the addition of thioacetamide and aged at 80 °C for 1.5 h, accompanied by vacuum drying for a long period. After that, a suitable amount of $Ni(NO_3)\cdot 6H_2O$ dissolved in ethanol was further added to the suspension of CNT@CoS in ethanol and left for observation for 3 h. The formulation of CNT@CoS/NiCo LDH was confirmed after the centrifuged product was dried.

Another approach for the comparative study of carbon composites with NiMn layered double hydroxide (LDH/rGO, LDH/CB, LDH/CNT, and LDH/CNT/rGO) grafted by the coprecipitation method was deeply studied by Li *et al.*[80] Initially, carbonaceous materials such as CB and CNT were pretreated with $K_2S_2O_8$ before integration with LDH and GO *via* the Hummers' method. The coprecipitation approach was employed to prepare the composite from a homogeneous $Ni(NO_3)_2$ and $Mn(NO_3)_2$ suspension dispersed in DI water with CB and continuous magnetic stirring. Then, ammonia was added under mild conditions, followed by stirring. The new formulations were converted to NiMn LDH/CB after the addition of ammonia to the above-mentioned mixture at room temperature and washing and drying at 80 °C. Similarly, other composites were fabricated, replacing CNT, rGO, and a mixture of CNT : rGO (1 : 1) and designed as LDH/CNT, LDH/rGO, and LDH/CNT/rGO, respectively. A super architecture of NiMn LDH/CNT hierarchical structure was invented by Zhao *et al.*[68] for flexible and portable electronic devices. Herein, the surface modification of CNTs was performed by refluxing in $HNO_3$ at 120 °C for 5 h, followed by washing with DI water. Then, the composite was prepared by the typical procedure involving the dispersion of treated-CNT in a salt solution of $Ni(NO_3)_2\cdot 6H_2O$ and $Mn(NO_3)_2\cdot 4H_2O$, followed by the addition of NaOH and $Na_2CO_3$ dropwise to the above-mentioned mixture under stirring for 12 h. The product was obtained after drying at room temperature for the growth of the LDH nanosheet matrix on the CNT surface.

(III) Reflux condenser system

The process of heating for a certain duration at a constant temperature in a chemical reaction that involves condensed vapor at the top cooling part of a condenser is known as reflux heating. This process is employed for synthesizing nanoparticles, nanocomposites, nanosheets, and nanorods in a simple,[81] cost-effective, lower energy requirement, no loss of solvent, and eco-friendly way.[82] Besides, the size, morphology, and structure of the product can be tuned by changing parameters such as the reaction time, temperature, and mass concentration in solution, which has attracted significant attention. In addition, this process supports efficient reaction, purified sample, controlled temperature, safety during exothermic reactions, and also prevents the loss of the solvents and reactants. Consequently, all these characteristics lead to better activity.

Li *et al.*[83] investigated the performance of nickel aluminum LDH and CNT for SC and asymmetric hybrid capacitor applications. In the first step, pristine CNT was changed into modified CNT by refluxing with $HNO_3$ at 120 °C for 6 h, and subsequently filtered, washed, and dried to produce negatively charged CNT. Secondly, AlOOH solution was prepared from $\gamma$-$Al_2O_3$ *via* a hydrolysis-reflux combined method and CNT suspended in DI water mixed with the AlOOH solution to form AlOOH in the CNT backbone. Then, the solution was refluxed at 100 °C, followed by filtration and washing to obtain the AlOOH/CNT composite. Again, it converted into $Al_2O_3$/CNT by aging at 700 °C in $N_2$ for 1 h. The final composite was obtained from a dispersion of $Al_2O_3$/CNT powder in water followed by the addition of $Ni(NO_3)_2\cdot 6H_2O$ and 50 mL $NH_4NO_3$. An aqueous ammonia solution was added dropwise to the above-mentioned solution to maintain pH = 7. Then, it was refluxed in a microwave reactor for 2 h and filtrated, rinsed, and dried at 70 °C.

A practical and emerging battery-type ternary nanocomposite electrode CNT/$Co_3S_4$@NiCo LDH was developed by Wei *et al.*,[61] suggesting its superior electrochemical performance for employment in the energy storage field. Step I involved the preparation of cubic ZIF-67 by the addition of $Co(NO_3)_2\cdot 6H_2O$ and 2-MIM in an aqueous CTAB solution under vigorous stirring. Then, the product was centrifuged, washed, and vacuum-dried. Step II involved the synthesis of hollow and cubic $Co_3S_4$. Here, thioacetamide and ZIF-67 were dispersed in ethanol under sonication, and solvothermal treatment was performed at 120 °C for 4 h to produce hollow and cubic $Co_3S_4$ after centrifugation, which was rinsed with alcohol and subjected to vacuum drying. The next step was carried out to obtain a hollow, cubic and core–shell structure of $Co_3S_4$@NiCo LDH from $Co(NO_3)_2\cdot 6H_2O$ and $Ni(NO_3)_2\cdot 6H_2O$, which were added to a dispersion of polyvinylpyrrolidone-functionalized $Co_3S_4$ in ethanol, followed by the addition of hexamethylenetetramine and trisodium citrate dissolved in the above-mentioned solution with stirring and placed in a refluxing oil bath for 2 h with vigorous stirring for the *in situ* growth of $Co_3S_4$@NiCo LDH. This was followed by centrifugation, ethanol rinsing and drying at 70 °C. Finally, NiCo LDH@$Co_3S_4$/CNT was harvested from different mass ratios of CNT and $Co_3S_4$@NiCo LDH dispersed in a mixture of $H_2O$ and ethanol with stirring, followed by centrifugation, washing with ethanol, and drying at 70 °C for 12 h.

In the article by Yu *et al.*,[72] they described the synthesis of transition metal-based ternary NiCoAl LDH combined with various carbon nanohybrid materials as potential pseudocapacitor electrode materials. Firstly, CNTs were modified by acid oxidation by dispersing them in DI water under ultrasonication for 30 min, and GO was manufactured using the modified Hummers' method. Also, $NiCl_2\cdot 6H_2O$, $CoCl_2\cdot 6H_2O$, $AlCl_3\cdot 6H_2O$, and urea were mentioned as raw samples for the preparation of the ternary composite LDH. Henceforth, they were dispersed in DI water under ultrasonication containing individual specified carbon materials including CB, CNT, GO, or CNT/GO. Then, a desired amount of solution was refluxed at 180 °C with continuous magnetic stirring for 48 h, followed by filtration, rinsing with alcohol, and drying at 80 °C in the air for 12 h to create new pure LDH/CB, LDH/CNT, LDH/rGO, NiCoAl LDH/CNT nanohybrid composites, respectively.

The importance of the NiV LDH/CNT composite manufactured by Tu *et al.*[69] in a modified and facile single-step reflux method for asymmetric SC energy storage devices was demonstrated. The straightforward reflux approach needed the precursors of $NiCl_2 \cdot 6H_2O$, $VCl_3$, and urea, which were dissolved in water, followed by the introduction of CNT dispersed in $H_2O$ under sonication with vigorous stirring for 4 h. Then, the solution was transferred to a reflux system and heated at 105 °C for 24 h to obtain the NiV LDH/CNT hierarchical composition. Meanwhile, LDH/CNT and activated carbon inks were prepared in the protocol following the insertion of the LDH composite and acetylene black by the diffusion of PTFE in $H_2O$ and ethanol under continuous stirring until a homogeneous ink was formed.

(IV) Electrochemical deposition method

Electrochemical deposition or electrodeposition is a powerful, versatile, superficial, and established anticorrosion deposition technology,[84] spanning a range of nanocoatings to some millimeter-thick coating *via* redox reaction, which can be used as thermoelectric thin films with a uniform coating of metal oxides on a substrate by connecting an electric current in an electrochemical cell.[85,86] This ion/electron bottom-up nano-electrochemical deposition approach is also employed for the preparation of nanomaterials, nanowires, nanorods, and nanotubes, and also a convention for surface modification *via* surface charge, conductivity, and broad functional groups. In particular, it has gained more popularity due to its wide range of applications in laboratory research, the electroplating industry, decoration, protection of domestic applications, manufacturing of dies and molds, *etc.* Electrodeposition allows precise control of the thickness of the deposited layer with high purity and quality, enabling the creation of uniform coatings tailored to specific applications, *in situ* modification, incorporation of dopants, and cost-effective environmental support.

A fiber-shaped SC of NiAl LDH hierarchical electrode was developed on 3D CNT for practical and potential applications in energy storage devices through electrochemical deposition by Zhang *et al.*[87] Initially, a CNT dispersion was prepared using a suspension of sodium cholate and MWCNT in DI water under stirring at 80 °C, and then ground for 30 min. The carbon fiber (CF)@CNT composite was developed through the immersion of modified CF in a CNT dispersion for an impregnation time of 45 s and dried at 70 °C, resulting in CF@CNT. Then, an electrolyte containing 0.09 M $Ni(NO_3) \cdot 6H_2O$, 0.03 M $Al(NO_3)_3 \cdot 9H_2O$, and 0.45 M $KNO_3$ was deposited on CNT CF@layer at the cathodic potential of −1.0 V with varying deposition times, which was successfully represented as NiAl LDH/CNT@CF as the positive electrode and tremella-derived activated carbon with CF as the anode to fix the novel LDH/3D CNT nanocomposite.

In a study, the rGO–FeO–CNT–NiFe LDH electrode was adopted as the anode and AC-NiO as the cathode by Hsiao *et al.*,[66] revealing the electrochemical preparation of a composite *via* a hydrothermal, CVD, and electrodeposition process. The synthesis of the GO solution was carried out using a modified Hummers' method. The rGO–FeOOH combination was synthesized from oyster shell powder and iron sulfate powder added to GO solution and subjected to a hydrothermal process at 180 °C for 12 h, and subsequently freeze-drying. Then, CNT was deposited on rGO–FeOOH *via* chemical vapor deposition and transferred to a tube furnace. FeOOH decomposed into $Fe_2O_3$ and further reduced to FeO under acetylene gas flow. It also acted as a catalyst for the growth of CNT on rGO–FeO at different temperatures. Then, rGO–FeO–CNT was converted into electrodes under heating at varying temperatures in a slurry of polyvinylidene fluoride, rGO–FeO–CNT, and carbon black and dried at 120 °C for 12 h to provide the maximum surface area for redox activity.

NiFe LDH was constructed from a dispersion of its precursors of 0.15 M $Ni(NO_3)_2 \cdot 6H_2O$ and 0.15 M $Fe(SO_4)_2 \cdot 7H_2O$ in DI water. Then, NiFe LDH was electrolytically deposited on rGO–FeO–CNT-700 (where 700 °C represents the CVD temperature) at the potential of −1.0 V employing rGO–FeO–CNT-700, Ag/AgCl, and Pt wire as the working, reference, and counter electrodes, respectively, showing that rGO–FeO–CNT-700–NiFe LDH exhibited a synergistic effect in energy capacity.

Again, Zhao *et al.*[88] explored the development of high-performance NiCo LDH on mono-dispersed CNT coaxial layer on a carbon fiber substrate as the cathode and tremella-derived activated carbon as the anode material, which exhibited excellent electrochemical properties for application in both flexible and asymmetric SCs. The merit of this synthesis is the completely eco-friendly electrodeposition method. The precursors were 0.04 M $Ni(NO_3)_2 \cdot 6H_2O$ and 0.06 M $Co(NO_3)_2 \cdot 6H_2O$ solutions, which were electrodeposited on a CNT layer at a cathodic potential of −1.0 V for a varying deposition times, resulting the formation of NiCo LDH. Previously cleaned CFs dispersed in CNT were electrodeposited with LDH several times to explore optimized [NiCo LDH/CNT]@CF different-layered electrodes. Then, the anode material of tremella-derived activated carbon on CF was prepared using a tremella precursor and $KNO_3$ by mixing well and heating at 700 °C, 800 °C, and 900 °C for 2 h. Subsequently, this AC was washed in HCl and $H_2O$, denoted as TDC, and mixed with carbon fiber and PVDF in *N*-mehyl-2-pyrrolidone to form a slurry and further coated on CF to form the TDC@CF composite.

Also, Zhu *et al.*[89] described the preparation of a core–shell nanotube architecture of NiCo LDH@CNT on CFs *via* hydrothermal treatment and electrodeposition for application in energy storage and conversion devices. In this approach, the authors showed the preparation of ZnO nanorods on the surface of CF *via* a hydrothermal approach and porous interface layered with ion exchange CNTs was derived from ZIF-8 and grown on carbon fiber *via* hydrothermal treatment at 300 °C, resulting in a shorter electron pathway and ion diffusion route. Then, the composite of LDH/CNT was manufactured from raw materials of nickel nitrate hexahydrate and cobalt chloride hexahydrate dispersed in water, and for electrochemical deposition, CF with hollow CNT, calomel electrode, and Pt plate acted as the working electrode, reference, and counter electrode, respectively. Then, CF@CNT was deposited at the cathodic potential of −1 V for different deposition times to

obtain the NiCo LDH@CNT pristine electrode, which was further rinsed and dried.

The hierarchical NiGa LDH grown on *in situ* CNT was effectively employed to fabricated high-performance SC electrodes, as discussed by Li *et al.*[67] through four chemical synthesis routes. The preparation of NiGa LDH/CNT/carbon cloth (CC) involved four steps. Initially, FeOOH/CC was derived by soaking CC in ferric nitrate and sodium sulfate dispersion in water. Then, it was aged in a Teflon-lined autoclave at 120 °C for hydrothermal treatment, followed by washing with DI water and drying. Then, Fe-MOF/FeOOH/CC was prepared through coprecipitation by adding 2-methylimidazole and FeOOH/CC in methyl alcohol. Next, Fe-MOF/FeOOH/CC was heated at high temperature under Ar, and the product was immersed in HCl solution, followed by rinsing with water many times to fabricate hollow CNT/CC *via* carbonization. Finally, the unique design of the asymmetric SC electrode NiGa LDH/CNT/CC was obtained using precursors of a hydrated compound of both nickel nitrate and gallium nitrate dispersed in water for electrodeposition at a deposition voltage of −1.0 V in a range of deposition times, where CNT@CC was assembled as the working electrode, a saturated calomel electrode was used as the reference electrode and Pt as the counter electrode (Fig. 5).

(V) Chemical deposition

This type of deposition involves a reaction in which vapors or gases are deposited on a solid substrate by a current flow into a liquid/electrolyte containing dispersed charged particles. Therefore, it has more advantages than chemical reactions. The resulting solid material may be formed as uniformly coated thin films and single crystals and its thickness controlled to the atomic or molecular level, with high purity, nanostructured blend films, or nanoparticles, and this method is environmentally friendly.[90,91] A wide range of physical, chemical, and tribological properties can be studied by varying the substrate, substrate temperature, liquid composition, and purging gas. This process is more economical than other processes given that no high temperature or pressure is required for this pioneering synthesis.[92] This method is broadly divided into chemical vapor deposition and chemical bath deposition.

The design of high energy density, high surface area, and excellent electrochemical performance NiCo LDH nanoflakes directly grown on CNT through a simple chemical deposition method was studied by Chen *et al.*[93] to produce a low-cost performance pseudo-SC. Specifically, a piece of CNT was immersed in a solution of $NiCl_2$ and $CoCl_2$ in water with a total concentration of 1 M, followed by the dropwise addition of ammonia until the pH became 9. After mixing for 3 h, the sample was rinsed with water and ethanol and dried for 48 h, generating a nanoflake structure of NiCo layered double hydroxide on carbon nanotube with electrochemical stability.

(VI) Solvothermal process

This type of synthesis of nanomaterials is performed in a nonaqueous solution at elevated temperature and pressure. The materials are transferred to Teflon-lined autoclave vessels above their boiling point to explore sanitary, moisture, and contaminant-free, as well as free from structural and chemical defects to achieve an appropriate degree of crystallinity, pore size, shape, and crystal morphology.[94] This process is used to prepare various NPs, including single crystals, thin films, 1D wires, 2D nanorods, and 3D spheres, owing to its many advantages such as easy, green, cost-effective, fast synthesis of crystalline structures and stable materials, with low power utilization.

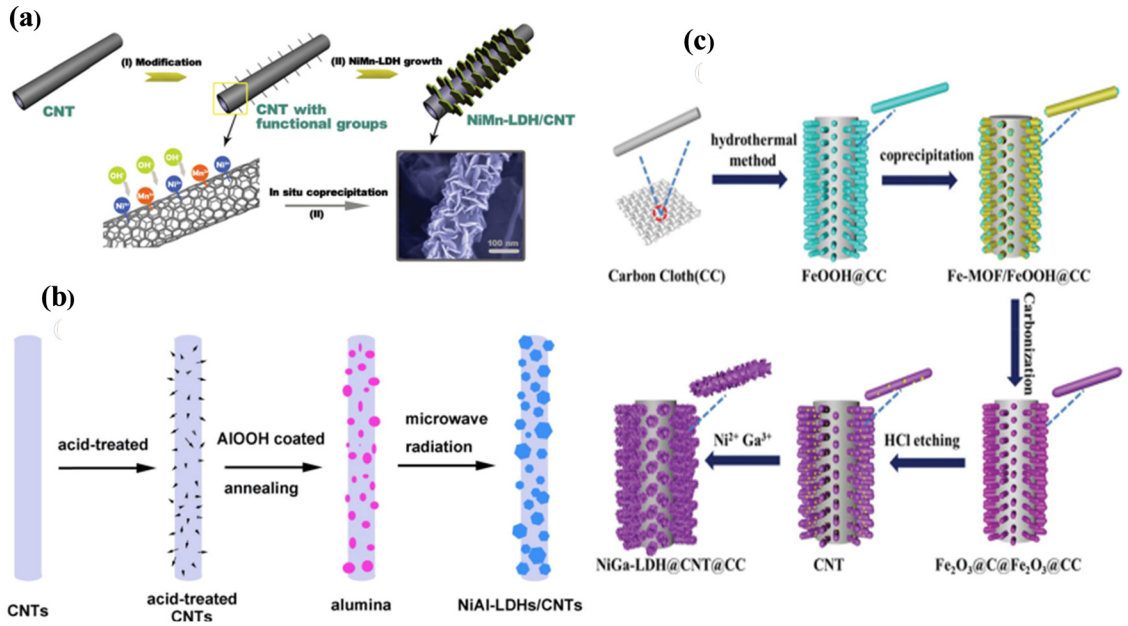


Fig. 5 (a) The NiMn LDH/CNT composite electrode synthesis method. Reproduced with permission from ref. 68. (b) Schematic representation of the NiAl LDH/CNT composite. Reproduced with permission from ref. 83. (c) Illustration of the preparation of NiGa LDH/CC. Reproduced with permission from ref. 67.

Therefore, this novel approach plays a significant role in diverse of research fields ranging from biomedical applications, sensors, photocatalysis, electrocatalysis, and crystal growth to energy storage and its conversion.[95]

The synthesis of a three-dimensional flower-like architecture of NiAl LDH/CNT combined with reduced graphene oxide sheets (GNS) *via* a single-step ethanol solvothermal process was demonstrated by Yang *et al.*[57] The superficial electrode was composed of raw materials of $Ni(NO_3)_2{\cdot}6H_2O$, $Al(NO_3){\cdot}9H_2O$, and urea dissolved in ethanol with continuous magnetic stirring and further transferred to an autoclave at 140 °C. Then, the sample was washed with water and alcohol and dried after cooling to obtain the host NiAl LDH. Then, a mixture of $Ni(NO_3)_2$, $Al(NO)_3$, and urea was poured into a dispersion of a specific amount of GNS, which was prepared from GO and CNT in ethanol with continuous stirring through a solvothermal approach at 140 °C to establish the new ternary nanocomposite NiAl LDH/CNT/GNS by controlling the ratio of GNS and CNT.

(VII) Thermal chemical vapour deposition (TCVD)

TCVD is a sub-technique that belongs to the chemical vapor deposition family in which atoms or molecules in gaseous form coat a solid thin film through the excitation of thermal energy. The gases are decomposed into atoms or molecules at high temperatures and coated on the surface of the high-temperature substrate. The uniqueness of this process is that it is a simple, environmentally friendly, and single-step process for designing CNTs, graphene, deposition of carbides, nitrides, and borides on respective electrodes, and multilayer films can be produced by changing the reactant gases.[96,97]

A 3D core shell of NiCo LDH was combined with CNT and nickel foam as the positive electrode and activated polyaniline-derived carbon (APDC) was employed as the negative electrode in the study by Li *et al.*[98] for the fabrication of advanced asymmetric SCs. The first step involved the preparation of APDC from PANI (polyaniline)-derived carbon, which was heated at 700 °C for 1 h, followed by heating in an aqueous KOH solution.

In the next step, a CNT layer was grown on cleaned nickel foam (NF) through a thermal chemical vapor deposition process by passing Ag gas into the furnace at 600 °C, and subsequently cooling. Then, the electrolyte solution containing 0.1 M $Ni(NO_3)_2$, 0.2 M $Co(NO_3)_2$, and 0.75 M $NaNO_3$ was electrodeposited at the cathodic potential of −0.7 V on an electrochemical workstation to deliver the NiCo LDH@CNT/NF conductive electrode after washing with DI water and drying.

### 4.2 Physico-chemical techniques

Several techniques have been employed to confirm the formation of materials, including phase identification, surface topography, and electrochemical studies, as noted in Table 3, together with supporting information and the scientific tools used.

The physicochemical properties of synthesized CoAl LDH/CNT power were analyzed by XRD, SEM, and XPS, as reported by Zhang *et al.*[2] The diffraction peaks of CoAl LDH/$gC_3N_4$, CoAl LDH/CNT, and CoAl LDH/AC located at $2\theta$ = 11.5°, 23°, 34.48°, 39°, 46°, 59.9°, and 61.45° correspond to the Bragg planes at (003), (006), (012), (015), (018), (110), and (113), respectively, as shown in Fig. 6(a) and (b). The intensities of the peaks were high, indicating the maximum degree of crystallinity. Moreover, the (003) and (006) planes show the direction of crystal growth and single phase, and the extra carbon peaks proved that the linking between the LDH and carbon materials was perfect. The surface morphology and pore size were characterized by electron microscopy images, which confirmed the presence of ultrathin nanosheets of all three carbon composites with LDH. The aggregation between two nanosheets was optimized and greatly influenced the electron transport. A further XPS study was carried out, showing the electronic transition of CoAl LDH/activated carbon at 284.8 eV for $sp^2$ hybridized carbon element and the spectra of Co split at the binding energies of 781.77 eV and 797.7 eV as $2p_{1/2}$ and $2p_{3/2}$ subshell transitions, respectively. Yang *et al.*[72] arranged a CoAl LDH/CNT composite and carbon nanohorns *via* the hydrothermal

Table 3 List of experimental characterization techniques used for the synthesis of SC electrodes

| S. no. | Name of tool | Type | Supporting information | Ref. |
|---|---|---|---|---|
| 1 | X-Ray diffractometer | Analytical instrument | Lattice and crystal structure | 2, 70, 75 and 87 |
| 2 | Electron microscope | Imaging tool | Surface morphology including pore size and shape | 62, 63, 72 and 87 |
| 3 | Transmission electron microscopy | Imaging tool | Inner shell surface structure | 62, 75 and 87 |
| 4 | Fourier transform infrared spectrometer (FTIR) | Analytical instrument | Chemical bond and functional group | 7, 62 and 70 |
| 5 | Raman spectrometer | Analytical instrument | Chemical composition | 7, 57 and 66 |
| 6 | X-Ray photoelectron spectrometer (XPS) | Analytical instrument | Chemical and electronic state of atom, atomic ratio | 57, 59 and 69 |
| 7 | Brunauer–Emmett–Teller (BET) | | Specific surface area | 57 and 70 |
| 8 | Electrochemical workstation | Cyclic voltammetry | Identification of anodic and cathodic peak | 57, 59 and 69 |
| 9 | Electrochemical workstation | GCD (galvanostatic charging–discharging) | Specific capacitance | 57, 59 and 69 |
| 10 | Electrochemical workstation | Ragone plot | Electrostatic discharge energy | 62, 66 and 75 |
| 11 | Electrochemical workstation | Electrochemical impedance spectroscopy (EIS) | Equivalent series resistance | 57, 59 and 70 |

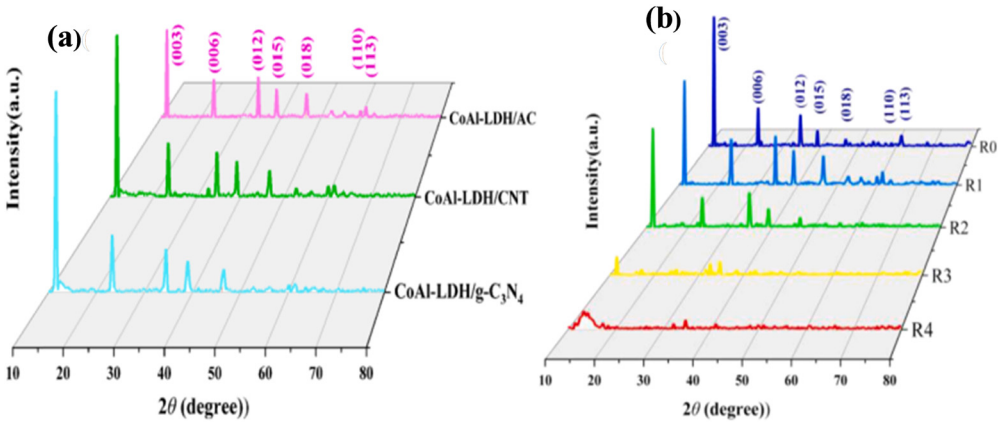


Fig. 6 (a) XRD spectra of CoAl LDH/AC, CoAl LDH/CNT, and CoAl LDH/g-$C_3N_4$. (b) XRD pattern of CoAl LDH/AC at different ratios. Reproduced with permission from ref. 2.

route. The X-ray diffraction pattern of LDH matched the corresponding JCPDS No and the narrower peak at 26° corresponds to the (002) plane for CNT and super P carbon, indicating their high crystallinity and small size. Similarly, the XRD pattern of rGO matched the plane crystal (002) of graphite. The chemical composition of LDH was investigated by FTIR, with the peaks in its spectrum at 3480, 1638, and 1368 $cm^{-1}$ corresponding to the metal–OH stretching, H–O–H bending at the interlayer, and asymmetric vibration of the C–O bond, respectively. Therefore, both the XRD and FTIR analyses confirmed the LDH formation with absolute accuracy. Again, the analytical Raman spectra revealed two major characteristic peaks of carbonaceous materials at 1350 $cm^{-1}$ and 1590 $cm^{-1}$ for the D and G bands, respectively. Fig. 7(a)–(c) show the hexagonal morphological structure of CoAl LDH and carbon additives (CNT/CNH) with simple flower- and fiber-like structures, respectively, and Fig. 7(d) shows their good electrical conductivity. Also, the maximum surface area per unit mass, which allows accessible electron/ion transportation channels, is shown in Fig. 7(e).

Further characterization of the CoAl LDH/CNT composite was performed by Yu *et al.*[73] The peak intensity for the (003) and (006) planes in the LDH composite with CNT diminished in comparison to the pre- and post-treated LDH with aqueous solution because the peak due to hydrotalcite disappeared after shaking with formamide, proving the formation of single nanosheets. As in the previous literature, the material structure was hexagonal according to the SEM images, and a curled nanosheet stacking of pristine LDH was observed. However, a rupture was observed in the LDH/CNT composite. Also, TEM

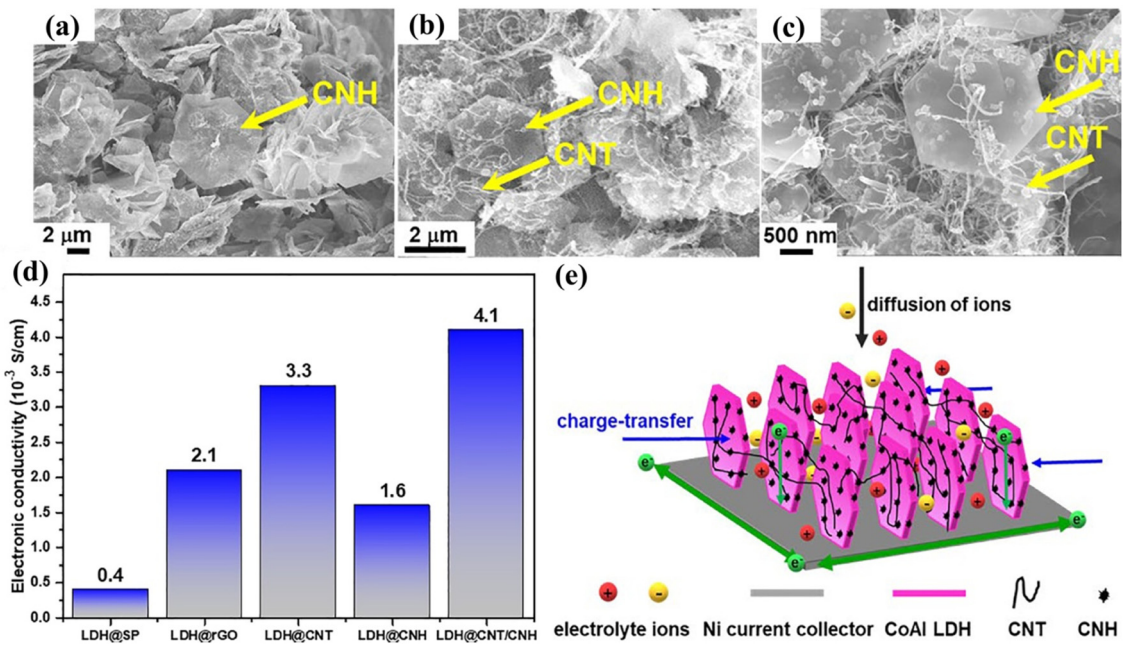


Fig. 7 SEM images of (a) CoAl LDH CNH and (b) and (c) CoAl LDH CNH/CNT. (d) Electrical conductivity of LDH prepared using different additives. (e) Schematic representation of the electrolyte ion diffusion path in LDH and CNH/CNT electrodes. Reproduced with permission from ref. 72.

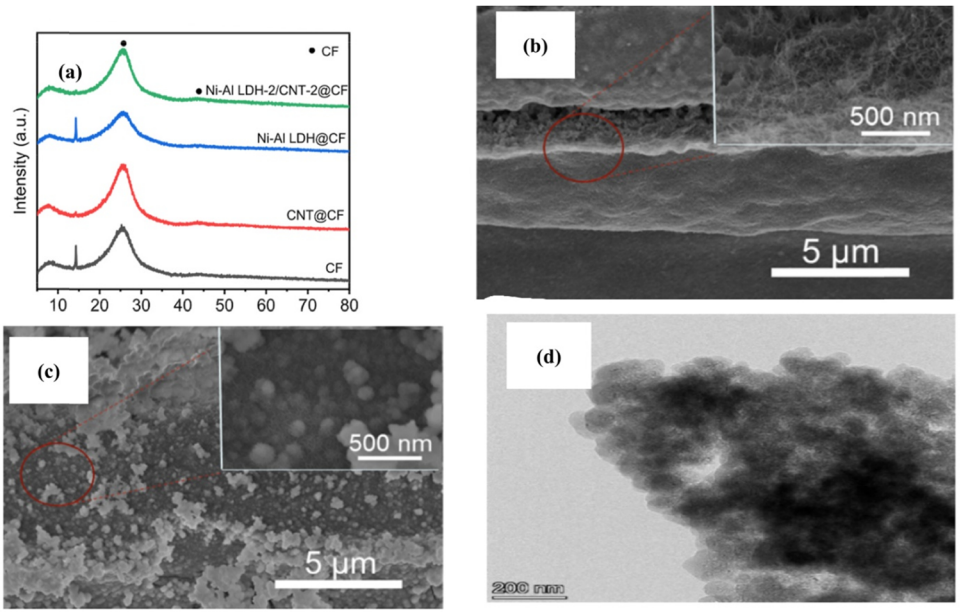


Fig. 8 (a) XRD patterns of CF, CNT/CF, LDH/CF, and LDH/CNT//CF. SEM images of (b) LDH/CNTs and (c) LDH/CNT@CF. (d) TEM analysis of LDH/CNT@CF. Reproduced with permission from ref. 87.

revealed the presence of ultrathin nanosheets in the composite, which increases the area for contact with the electrolyte ions. Therefore, CoAl LDH/CNT is a better candidate for electrochemical study than pure LDH. Again, the chemical investigation was performed by X-ray photochemical spectroscopy using the charge potential model, that is, the BE of the composite increased due to the positive charge of CNT on LDH, which validates the formulation of LDH/CNT, a 3D core–shell structure of CoNi LDH tied on N-doped carbon coated (N-CNT) *via* the hydrothermal route, as reported by Liu *et al.*[58] According to the XRD analysis of both N-CNT and composite, both samples possess the characteristics peak at 26° for the (002) crystal plane, showing the presence of hexagonal graphitic carbon due to CNT. The other crystal planes correspond to the hydrotalcite LDH phase, confirming the successful combination of the LDH shell and N-CNT core. The SEM images validated the vertical growth of LDH on N-CNT as the core–shell engineered architecture. Also, TEM verified the 3D core–shell structure and authenticated the absence of nanosheet stacking and large surface area for an increased number of active sites, promoting the electrochemical redox activity. Similarly, XPS confirmed the chemical composition of Co, Ni, O, N, and C elements, which was consistent with the XRD pattern. The results for CoNi LDH/CNT showed the splitting of Co $2p_{3/2}$ and Co $2p_{1/2}$ at the BE 781.2 eV and 796.6 eV, respectively, creating a spin energy separation of 15.4 eV. This indicates the oxidation state, similar to the case of the Ni-splitting satellite peaks. These concepts are clear with the XRD validation for successfully synthesizing LDH/CNT. The synthesis of carbon fiber (CF), CNT@CF, NiCo LDH@CF, and NiCo LDH-CNT@CF was reported by Zhang *et al.*[87] *via* the electrodeposition process and the lattice phases were identified by X-ray diffraction analysis. Fig. 8(a) shows the strong peak at 25.5° and 43.8°, referring to CF and CNT@CF, respectively. An impurity was detected, which had no impact on the sample composite, and all the strong diffraction peaks indicated that this composite is potential candidate to investigate its overall performance. The CNT nanoparticles were completely and continuously adhered to the NiAl LDH ultrathin sheets, which could prevent their structural damage, according to the SEM analysis, as shown in Fig. 8(b) and (c). The second layer showed a nano flower-like morphology with a CNT NP network. Alternatively, the TEM image, as shown in Fig. 8(d), demonstrated irregular hexagonal-like structure features with an interplanar distance 0.26 nm (Fig. 9(a)), corresponding to the (012) plane of NiAl LDH, and Fig. 9(b) shows the high-resolution TEM image. The presence of Ni, Al, O, and C was authenticated by the energy dispersive X-ray mapping (EDS), as shown in Fig. 9(c). Fig. 9(e) confirms the electronic and valence state of the elements according to the XPS analysis. The C 1s spectra show three peaks at 284.8 eV, 285.6 eV, and 287.8 eV, corresponding to C═C, C–O, and C═O, respectively, showing the presence of oxygen-containing functional groups in NiAl LDH/CN. The O 1s, Al 2p (Fig. 9(d)), and Ni 2p (Fig. 9(f)) spectra were recorded, indicating the interconnection between LDH and CNT by smooth electrodeposition, and further the crystal structure and morphology of the surface to react with electrolytic ions, which can reduce the paths for electron/ion movement in the electrochemical cell. Thus, it will promote fast charge transfer, indicating better energy storage ability.

Hsiao *et al.*[66] described the electrochemical deposition of NiFe LDH on rGO–FeO–CNT to prepare rGO–FeO–CNT–NiFe LDH as the negative electrode and AC/NiO as the positive electrode, thereby enhancing the electrochemical properties in an asymmetric supercapacitor. According to the analysis of rGO–FeO–CNT by X-ray diffraction, the peak at 26.6° corresponds to the (002) plane of CNT, as shown in Fig. 10(a). Also, $CaSO_4$ was found

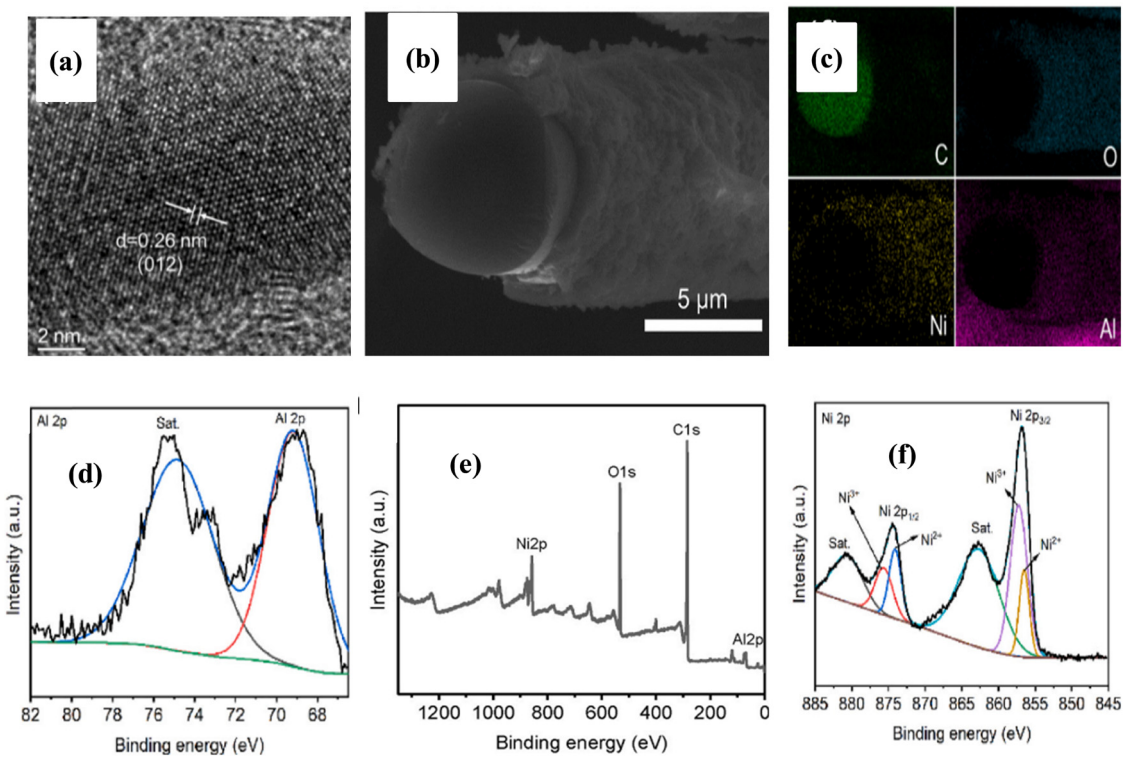


Fig. 9 (a) TEM image of NiAl LDH/CNT@CF. (b) EDS image and (c) corresponding color mapping. XPS spectrum of (d) Al 2p, (e) LDH/CNT@CF and (f) Ni 2p. Reproduced with permission from ref. 87.

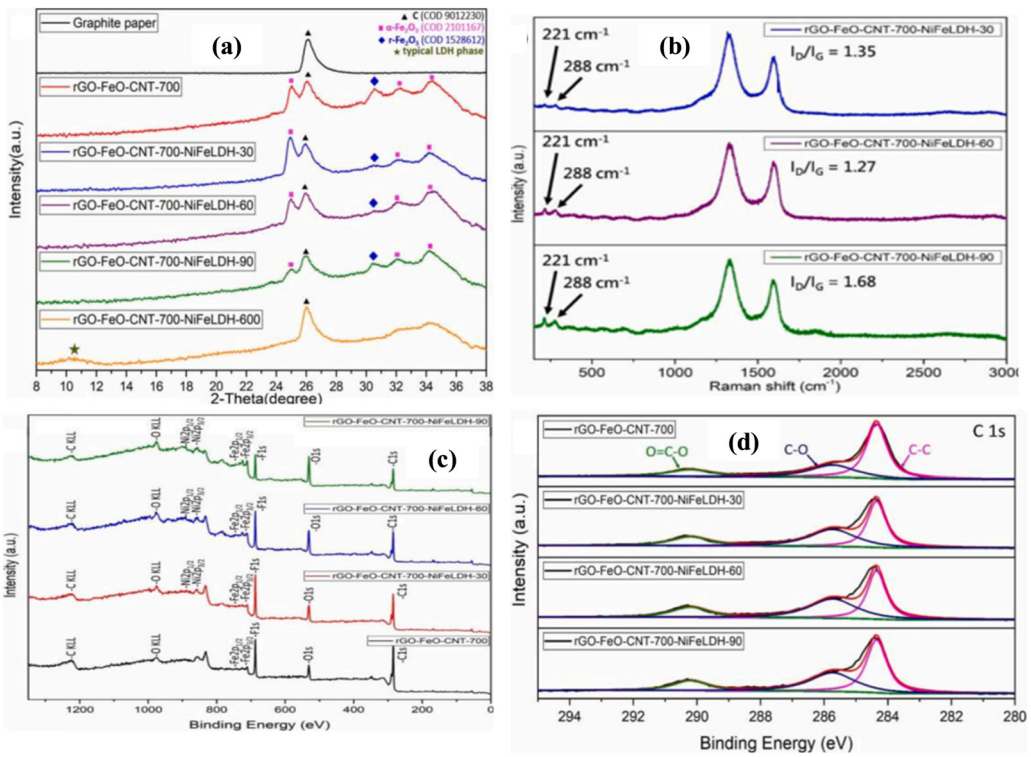


Fig. 10 (a) Small-angle XRD patterns. (b) Raman spectra of electrodes electrodeposited at different times. XPS spectra of (c) different rGO–FeO–CNT–NiFe LDHs and (d) C 1s. Reproduced with permission from ref. 66.

given that this powder was collected from oyster shells, which reacted with $SO_4^{2-}$ ions in solution to form $CaSO_4$. Then, a small-angle X-ray scattering (SAXS) experiment was conducted for the pristine LDH, $Fe_2O_3$, and the composite to determine their phases and crystallinity. The diffraction pattern of the graphite and iron oxide phases was detected at the appropriate positions, and the crystal atomic plane of (003) indicates the presence of LDH. The surface morphology and size were illustrated in the FESEM and HRTEM images. FeOOH nanorods were reduced to ion clusters at different temperatures, and HRTEM revealed that CNT nanorods with a diameter of 700 nm were uniformly grown on the rGO ultra-thin sheets. There were clear visible of fragments of rGO–FeO–CNT aged at 700 °C uniformly grown on rGO nanosheets, acting as the electron transport path for conductivity. Similarly, the LDH thin layer was nearly 120 nm in the composite, as analyzed by high-resolution FESEM.

The chemical composition of rGO–FeO–CNT–NiFe LDH was described by Raman spectroscopy. The Raman spectra (Fig. 10(b)) showed peaks for $Fe_2O_3$ at 221 and 288 $cm^{-1}$, indicating two different modes. The D and G bands were estimated for the ordered and disorder carbon atoms in the composite. Moreover, the higher $I_D/I_G$ ratio at different temperature treatments showed the better-ordered structure of atoms, which means greater crystallinity, significantly enhancing the electron flow to the current collector *via* the electrode. Fig. 10(c) and (d) show the band energy, chemical bond, electronic state, and structural view obtained by full-range XPS scanning. The C 1s, O 1s (Fig. 10(a)), Fe 2p (Fig. 10(b)), and Ni 2p (Fig. 10(c)) spectra of rGO–FeO–CNT–NiFe LDH showed peaks at the binding energies of 284.4 eV, 531.5 eV, 710.8 eV, and 856.3 eV (BE), respectively. Alternatively, in the high-resolution XPS survey spectrum, the C, O, Fe, and Ni peaks split into a doublet around their spectral position. Again, the same elemental composition of the composite was also verified by the EDS analysis and high-angle annular dark field scanning transmission electron microscopy (HAADF-STEM).

In the report by Li *et al.*,[83] they prepared an NiAl LDH/CNT composite using a reflux system and explored the diffraction data, crystal structure, and phase of acid-treated CNT, AlOOH/CNT, $Al_2O_3$/CNT, and NiAl LDH/CNT. The XRD plot CNT was properly indexed to the (002) crystal plane at 26.1°, as shown in Fig. 11(a). Well-defined peaks for AlOOH/CNT and $Al_2O_3$/CNT were observed, but the characteristic peaks of the composite were determined with the *R*3*m* space group of the hydrotalcite structure. Also, the spectrum of CNT in the refined form in Fig. 11(b) reveals the FTIR vibrational peaks of acid-treated CNT and the composite electrode NiAl LDH/CNT. The peaks at 1384 $cm^{-1}$ and 3434 $cm^{-1}$ correspond to the N–O and $H_2O(OH^-)$ vibrational bonds at the interlayer of LDH and prove the presence of $NO^{3-}$ and $OH^-$ ions, and water molecules, respectively, strengthening its conductivity. XPS was also performed to study the composition of the LDH/CNT composite. Fig. 11(c) shows the Ni $2p_{1/2}$, Ni $2p_{3/2}$, O 1s, C 1s, N 1s, and Al 2p spectra, which agree with the FT-IR vibrational peaks. Fig. 11(d) shows two satellite peaks of Ni $2p_{3/2}$ and Ni $2p_{1/2}$ at 855.8 eV and 873.4 eV, respectively. The pore size of the material was

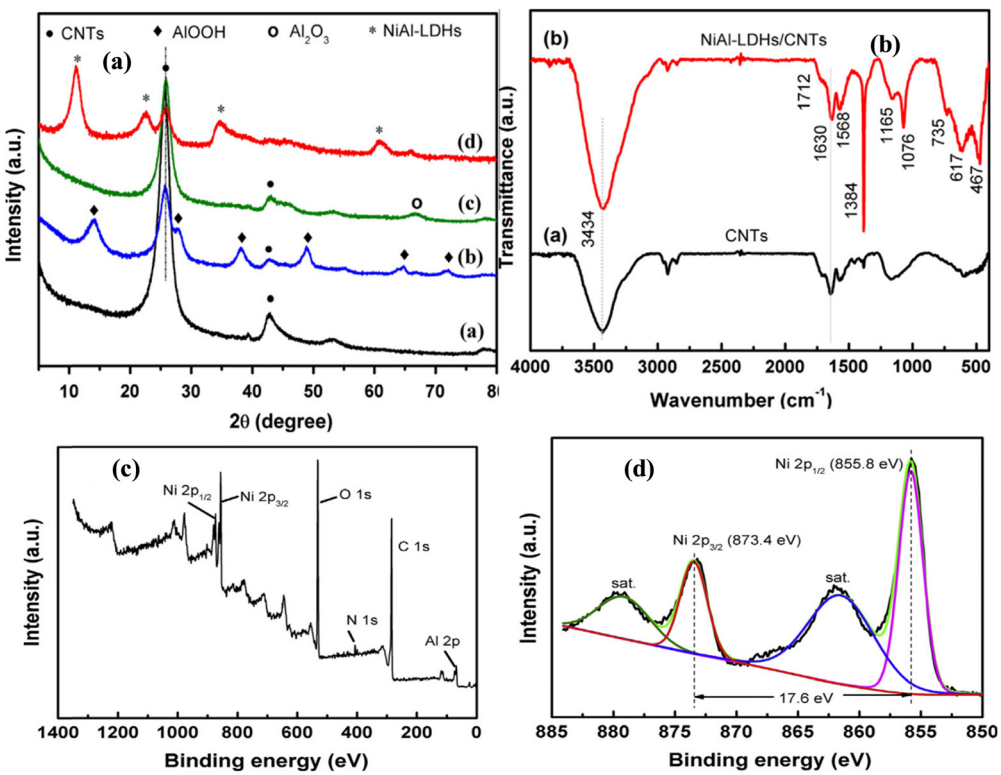


Fig. 11 (a) XRD analysis of CNTs and LDH. (b) FTIR spectra of CNTs and the LDH/CNT composite. (c) XPS analysis of NiAl LDH/CNT. (d) Ni 2p spectra of NiAl LDH/CNT composite. Reproduced with permission from ref. 83.

measured using its BET surface area, *i.e.*, 110 $m^2$ $g^{-1}$, which was one of the excellent results for faradaic redox reaction active sites in electrochemical cells. The SEM analysis revealed that the size of the nanorod of CNT was 20 nm, which agreed with the XRD plot. The LDH ultrafine nanosheets were connected with CNT in the composite, as observed by TEM.

## 5. Electrochemical applications of LDH/CNT

LDH/CNT-based supercapacitors are revolutionary devices with distinctive features for the fabrication of sustainable and clean energy storage system. Their storage capacity in nearly 100–1000-times per unit volume that of conventional capacitors. Also, their other advantage is the fast charging and discharging of the cell in a wide temperature range. These passive devices have greatly improved with the development of a wide variety of advanced materials and new innovative technologies. Moreover, their energy and power must be optimized to meet the power density, energy density and cycle life demands. These activities can be further improved by tuning LDH/CNT composites *via* research methodology and data available in the literature. Owing to the fact that the state of the art of the optimization performance metrics has been significantly investigated in the past few decades, it has been shown that their performance depends on various parameters. These parameters include novel architectural manufacturing, increasing the interfacial surface area, shorting the ion diffusion path and increasing the equivalent series resistance (ESR), self-discharge rate, specific capacitance, operating voltage and life cycle. Regardless of the conditions, the development of LDH/CNT nanocomposites should be easy, cost effective and support the significant collection of charged ions at the collector region to furnish the maximum energy of 0.5 $CV^2$ in units of joules.

Recently, Zhang *et al.*[2] designed CoAl LDH/g-$C_3N_4$, CoAl LDH/CNT, and CoAl LDH/AC nanocomposite electrodes for the fabrication of effective electrochemical supercapacitors. These innovative composites possessed a large surface area and abundant active sites, high electrical conductivity for the smooth charge process, and stability during faradaic reversible redox reactions. They showed the contribution of capacitance and diffusion properties of all types of electrodes. The extraordinary discharge-specific capacitance of CoAl LDH/AC varied from 1700 F $g^{-1}$ (850 C $g^{-1}$) to 1891 F $g^{-1}$ (946 C $g^{-1}$) according to the GCD plot. The $C_s$ values of other composited carbons were calculated. According to the EIS graph, the charge transfer resistance of LDH/g$C_3N_4$ is high, and its value is the smallest compared to the LDH/AC and LDH/CNT electrodes, as shown in Fig. 12(a) and (b). The AC composite showed the maximum surface area, number of active sites and porosity. The retention rate increased after 5000 cycles, which is one of the best flexible and wearable electrodes for energy storage SC materials, as shown in Fig. 12(c).

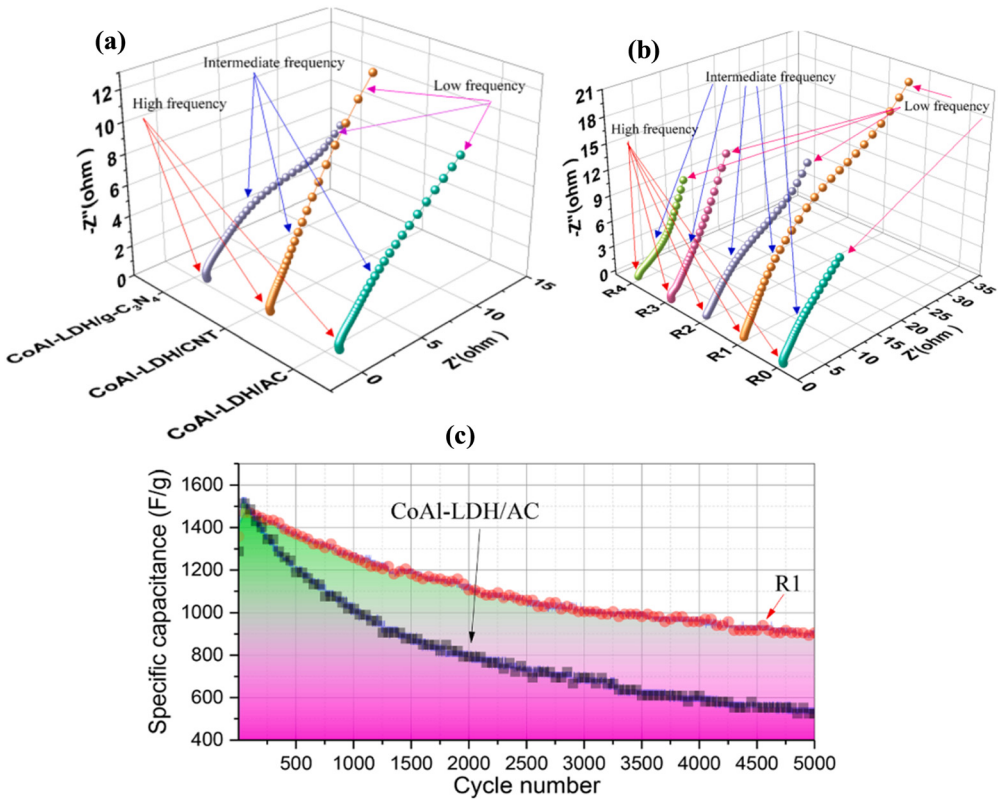


Fig. 12 (a) EIS graph of three electrodes. (b) EIS of the CoAl LDH/AC composite in different solvents. (c) Cycling stability of CoAl LDH/AC. Reproduced with permission from ref. 2.

The binding effect of CoAl LDH and carbon deployed as highly conductivities additives such as CNT and CNH (carbon nanohorn) effectively improved the electronic conductivity, as studied by Yang *et al.*,[72] which further built up the charge storage in a hybrid supercapacitor (HSC) by producing the largest enclosed area in the CV plot, as shown in Fig. 13(a)–(c). Also, the capacitance was calculated using the GCD plot (Fig. 13(d)), with highest $C_s$ of 754 F $g^{-1}$ or 125.7 mA h $g^{-1}$ at current density 1 A $g^{-1}$. Further, the newly developed accurate electrochemical cell provided a rate capability of 78.5% and 81.7% retention after 6000 cycles. The output of the device was calculated in terms of energy density and power density from the Ragone plot, *i.e.*, as shown in Fig. 13(e). The maximum energy density of 62.2 W h $kg^{-1}$ at the power density of 632.5 W $kg^{-1}$ was generated from CoAl LDH@CNT/CNH//AC in AC as the negative electrode and CoAl LDH@CNT/CNH as the positive electrode in the potential range of −1–0 V and 0–0.6 V in the electrochemical cell, respectively.

In addition, Yu *et al.*[73] reported the electrostatic connection between CoAl LDH and modified carbon nanotube developed *via* the hydrothermal approach to achieve an excellent electrochemical performed, in which the redox peaks increased at different scan rates due to conversion of $Co^{2+}$ to $Co^{3+}$ in the potential range 0 V to 0.6 V. Alternatively, the CV (Fig. 14(a)) area enclosed at a particular scan rate and the current of redox peak for the composite were much larger than that of the pristine LDH and CNTs, indicating its better electrochemical properties. Consequently, the composite delivered an average specific capacitance (Fig. 14(b)) of 884 F $g^{-1}$@current density of 0.86 A $g^{-1}$ with high retention rate characteristics of 88% after 2000 a long cycle life (Fig. 14(c)). Again, the Ragone plot (Fig. 14(d)) showed that the electrochemical cell had an energy density of 28 W h $kg^{-1}$@power density of 444.1 W $kg^{-1}$ in an essential asymmetric energy storage SC. The Nyquist plot of EIS (electrochemical impedance spectra) (Fig. 14(e) and (f)) was examined for a pure capacitive value of the composite than individual LDH and CNT, given that the EIS curve was closer to 90° and the diameter of its natural impedance curve was smaller than that of the others, representing its low charge transfer resistance. CNT possesses negligible resistance, chemical stability, and high conductivity and is employed for the fabrication of electrode materials with outstanding results. A 3D core–shell structure of CoNi LDH and nitrogen-doped CNT was designed by Liu *et al.*[58] to fill the gaps and opportunities in the field of SCs due to its high specific capacitance, large specific surface area per unit mass, maximum energy and power density, and electrochemical stabilization performance, as represented by the enclosed area in the CV (Fig. 15(a)) of the composite, which was greater than that of N-CNT and pristine LDH. The N-CNT/CoNi LDH composite showed a high specific capacitance, $C_s$, of 693 C $g^{-1}$ at a current density of 1 A $g^{-1}$ with 80% retention rate at 20 A $g^{-1}$ and 93% retention after 10 000 GCD (Fig. 15(b)–(d)). Also, its Ragone plot (Fig. 15(e)) showed the high energy density of 51.3 W h $kg^{-1}$ at the high power density of 533 W $kg^{-1}$ using N-CNT–CoNi LDH as the positive electrode and HPC (honeycomb porous carbon) as the negative

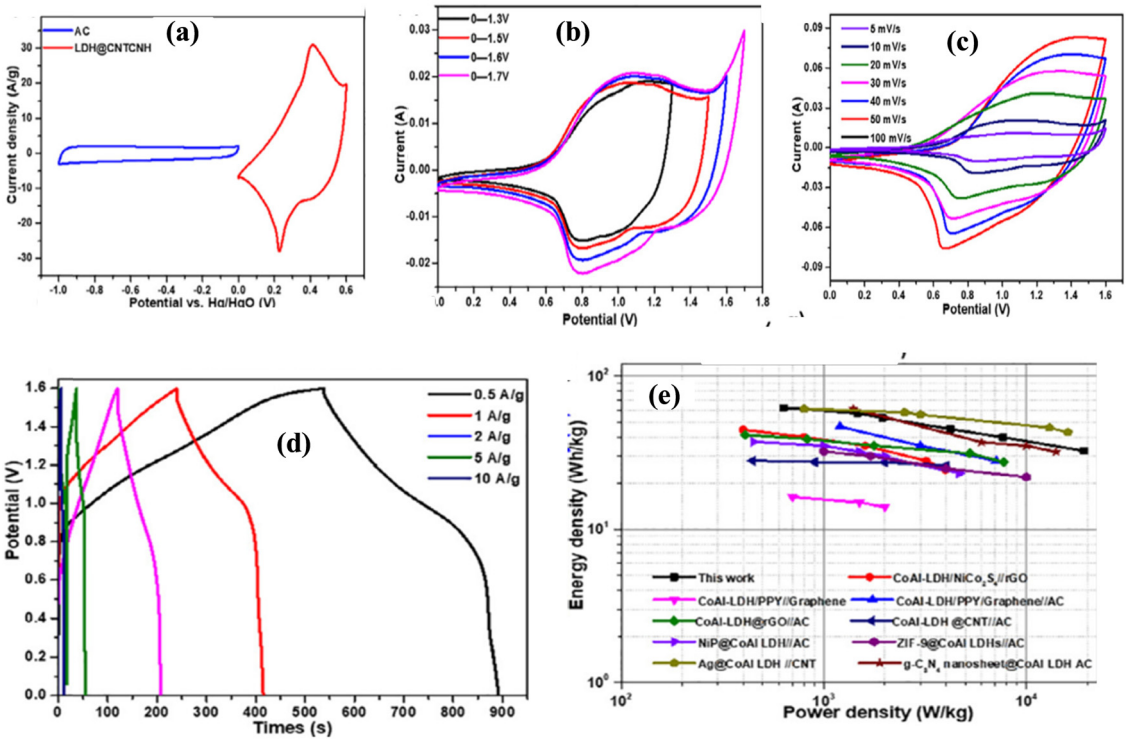


Fig. 13 (a) Cyclic voltammetry plot of LDH@CNT/CNH and AC. (b) CV plot of HSC device. (c) CV plot at different scan rates. (d) GCD plot at different current densities. (e) Ragone plot of the device. Reproduced with permission from ref. 72.

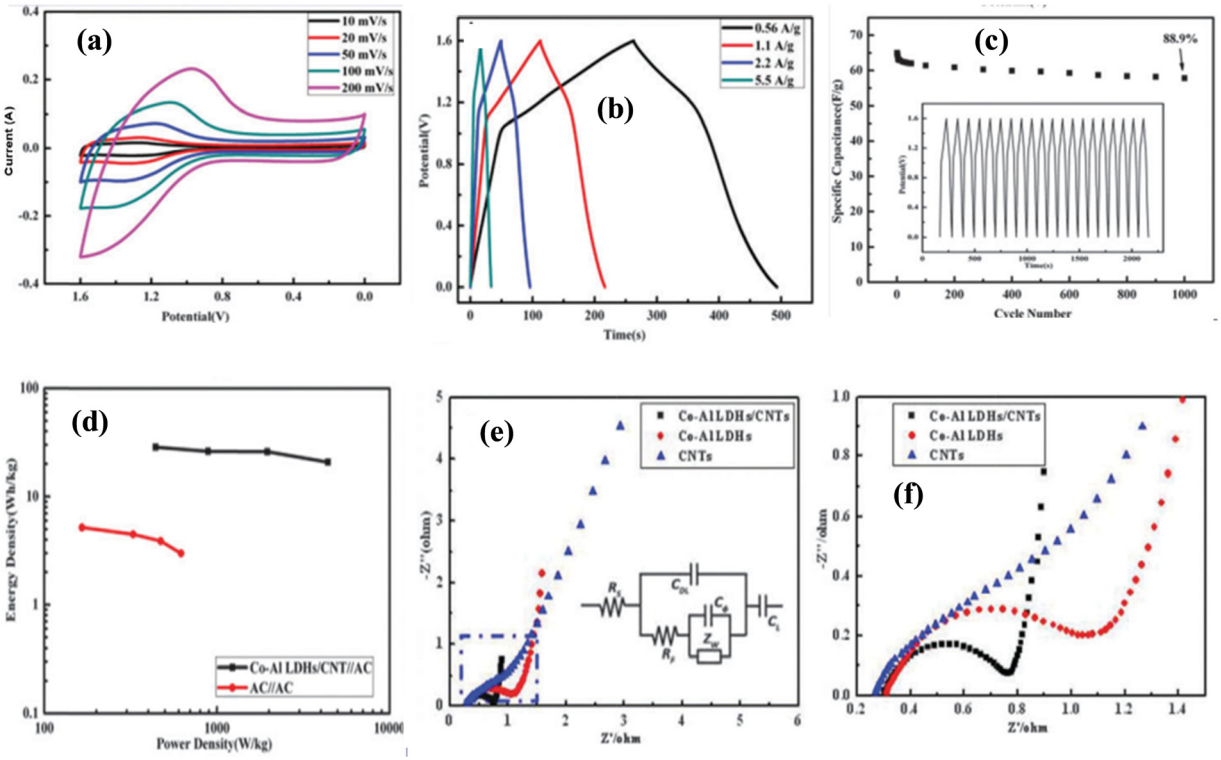


Fig. 14 (a) CV of asymmetric SC (CoAl LDH-CNT//AC). (b) GCD curve of CoAl LDH-CNT//AC. (c) Cycling stability. (d) Ragone plot of energy density *vs.* power density. (e) EIS spectra of CNTs, LDH, and LDH/CNT. (f) Magnified view of EIS. Reproduced with permission from ref. 73.

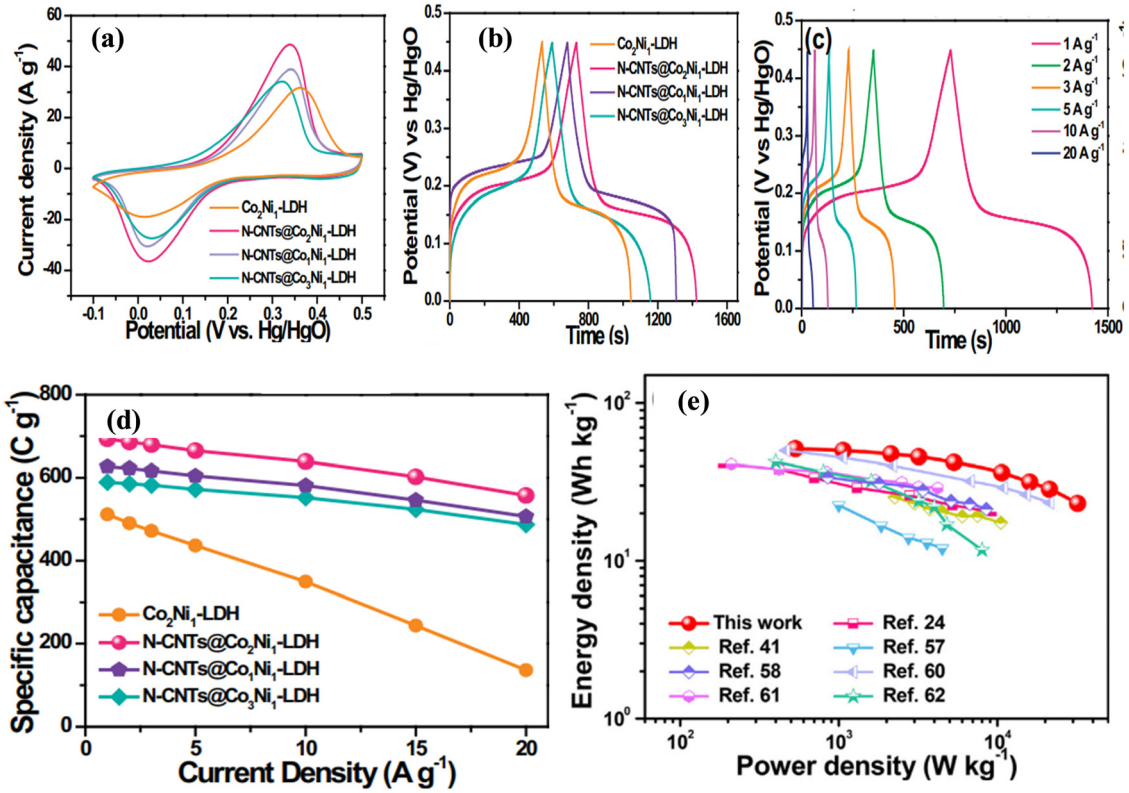


Fig. 15 (a) CV plot of different electrodes. (b) GCD curve of different electrodes at a fixed current density. (c) GCD curve of N-CNT–CoNi LDH. (d) Calculation of specific capacitance. (e) Ragone plot of the N-CNT–CoNi LDH-based asymmetric SC. Reproduced with permission from ref. 58.

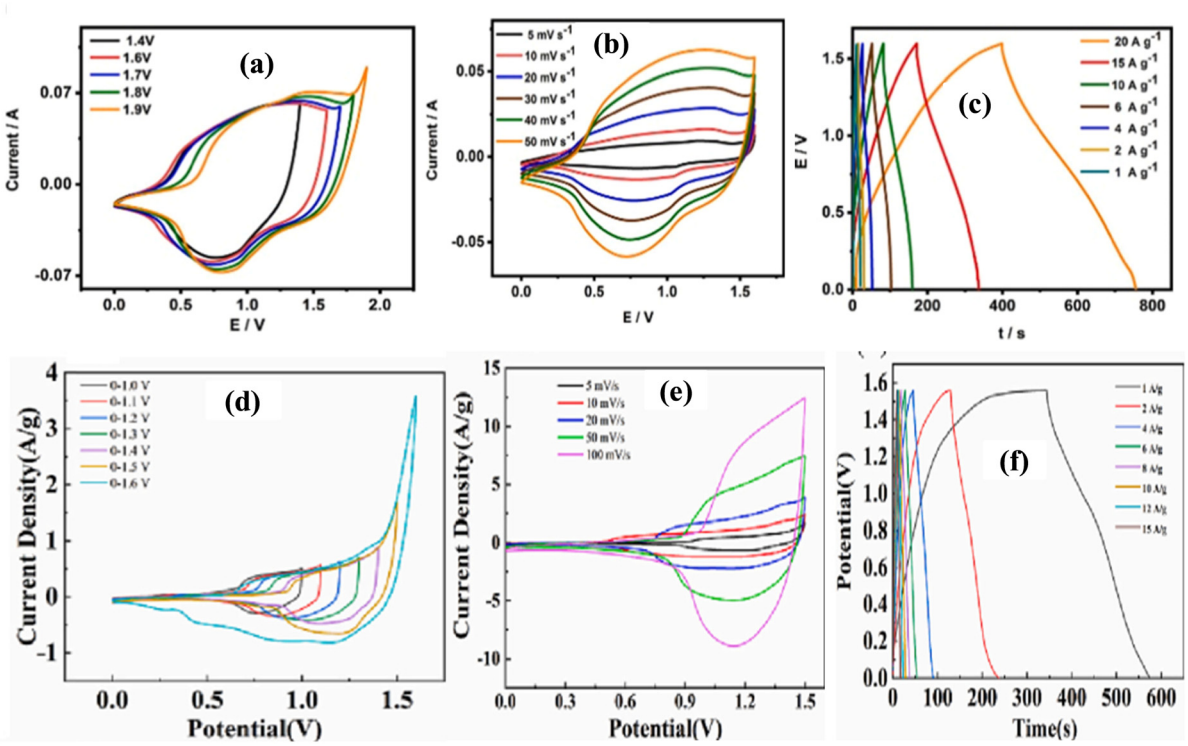


Fig. 16 (a) CV curves of the ASC cell in different potential windows. (b) CV curves of the ASC device at different scan rates. (c) CV curve of the ASC device at different current densities. Reprinted with permission from ref. 59. (d) CV curve of the CNF/CoNiFe (SDS)–LDH//AC ASC cell at different potential windows. (e) CV plot of CNF/CoNiFe (SDS)–LDH//AC at different scan rates. (f) GCD curve at various current densities. Reproduced with permission from ref. 62.

electrode, delivering excellent results for the constructed ASC (asymmetric supercapacitor).

A thorough discussion on the construction of CoNi LDH on a highly conductive MXene surface and multiwall carbon nanotube (MWCNT) for application as a high-performance novel electrode material in SCs was presented by Ma *et al.*[59] The MX–CNT–LDH composite showed the maximum integral area among the tested materials at 50 mV $s^{-1}$, suggesting its superior specific capacitance. Also, the CV (Fig. 16(a)–(c)) plots of the composite were measured at different scan rates. Moreover, the best specific capacitance result was 1382.2 ± 2 C $g^{-1}$ at 1 A $g^{-1}$ with a high capacitance retention of 96.7% for 6000 cycles. This ASC offered a high energy density of 78.7 ± 0.8 W $kg^{-1}$ at a power density of 800 W $kg^{-1}$, satisfying the most accurate result for building new asymmetric SCs. The article introduced by Ding *et al.*[62] on SDS incorporated CoNiFe LDH (SDS)/CNT, carbon black (CB), CoNiFe (SDS)–LDH, and carbon nanofibre (CNF)/CoNiFe (SDS)–LDH as novel composites for promoting asymmetric supercapacitors. The redox peaks and areal curves of the SDS-modified composites were calculated from their CV (Fig. 16(d) and (e)) plots. The carbon-based composite showed the maximum integral area and GCD curve (Fig. 16(f)), with the high capacitance of 193.9, 204.2, and 203. 3 mA h $g^{-1}$ at 1 A $g^{-1}$ for CB/CoNiFe (SDS)–LDH, CoNiFe LDH (SDS)/CNT, and (CNF)/CoNiFe (SDS)–LDH, respectively, with a retention of 71.3%. Among them, the ASC-based composite (CNF)/CoNiFe (SDS)–LDH//AC possessed the highest $C_s$ value of 148.1 F $g^{-1}$ at 1 A $g^{-1}$. The three ASCs showed excellent $C_s$, proving that they are prospective candidate electrode materials in the energy storage area. Luo *et al.*[78] introduced the conducting composite electrode material NiAl LDH and CNT using the coprecipitation approach to deliver its practical outputs in a symmetric SC after an electrochemical cell kinetic study. The solid-state supercapacitor showed the $C_s$ of LDH of 2447 F $g^{-1}$ at 2 A $g^{-1}$ with cycling stability of 90.1% after 2500 cycles. The leaf-like curve graph explained the pseudocapacitive attitude of the composite to determine its specific capacitance, ranging from 0.1 V to 0.4 V at different scan rates and current densities. Further, the faradaic pseudocapacitance and EDLC combination were verified from its GCD plot at different scan rates to deeply understand its usage in future generation SCs. All the graphs are presented in Fig. 17(a) and (b).

## 6. Other crucial conditions

The literature survey in Table 4 illustrates the properties, characteristics, and detailed features of several LDH/CNT nanocomposites manufactured *via* various routes. However, their discharge curves measured *via* chronoamperometry need to be explained. This behavior was studied by Lee *et al.*[99] by direct light incidents, which may result in low transport resistance and drastically enhanced ESD activities (electrochemical storage devices). This happens mainly in some cathodic materials,

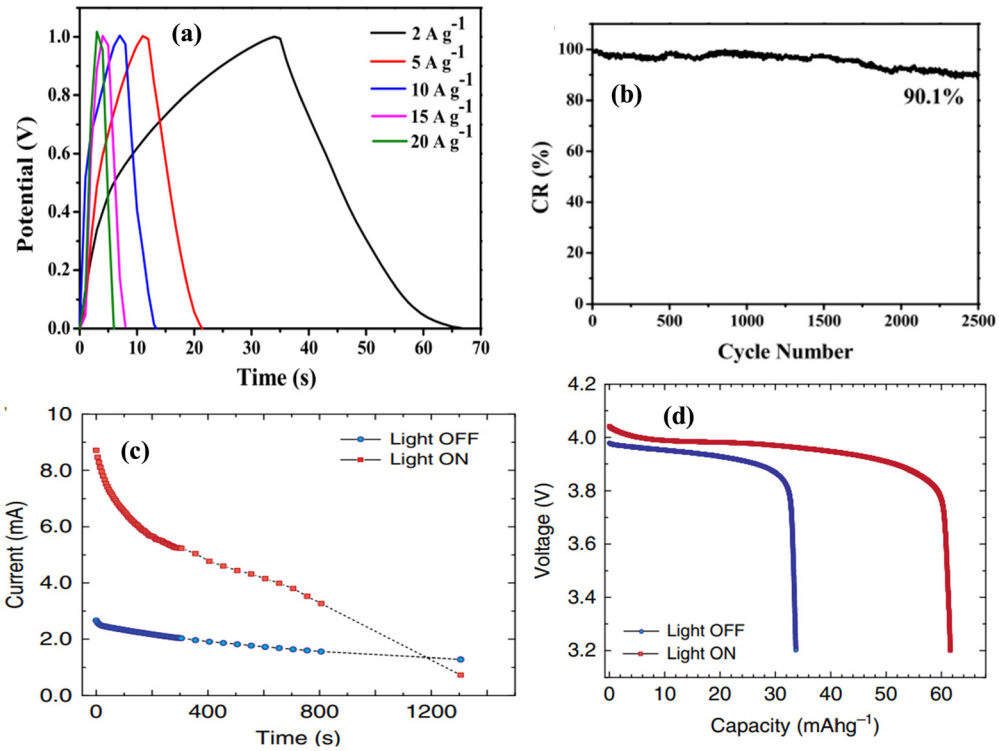


Fig. 17 (a) GCD curve of NiAl LDH/CNT at various current densities. (b) Retention of NiAl LDH/CNT is 90.1% after 2500 cycles. Reprinted with permission from ref. 78. (c) Chronoamperometry curve of the 'light-on' *vs.* 'light-off' state. (d) Discharge curve after chronoamperometry test. Reproduced with permission from ref. 99.

such as $LiMn_2O_4$, to create highly energetic electron–hole pairs sufficient to separate distinct charges, leading to a better charging rate, followed by massive energy storage at the collector region. Fig. 17(c) and (d) show the current generation and constant capacitance discharge curve from chronoamperometry for white 'light on' *vs.* 'light off' conditions.[99] Meanwhile, the applied electric field must be affected by the contribution of charge distribution in the electrolyte, in which the distribution of vanadium diselenide nanosheets ($VSe_2$) in sulphuric acid was verified to cause the fast migration of charged ions/electrons, better capacitance retention and hydrogen evolution reaction performance due to the presence of hydroxonium ions ($H_3O^+$) in the outer surface of the nanosheets when the voltage decreased from 126 to 70 mV. SCs are electrochemical cells with more advantages than batteries in terms of durability, wide operating temperature range, portability, chemical stability, power density, and charge/discharge rate. However, here, the temperature as a state variable affects the thermochemical and kinetic performance of the electrolyte, electrode, and storage devices. High-temperature storage equipment is impossible to achieve because the transport of ions will kinetically fail in the storage sites to acquire the maximum accessible area at high rates. For an example, Fletcher *et al.*[100] found that the electrolyte resistance and equivalent series resistance (ESR) decreased with an increase in temperature in the range of 15 °C to 40 °C and the ionic mobility increased in an ionic electrolyte EDLC cell containing activated carbon aerogel electrolyte; however, the capacitance increased after increasing the temperature of both the test cell and the commercial capacitor. Also, no reduction in capacitance was observed at lower temperatures, although there was an increase in the voltage window.

### 6.1 Environmental footprint and economic feasibility

Environmental footprint and economic feasibility of LDH/CNT composites: LDH/CNT composites are conventional materials, considering their production, processing, and transportation and the rich source of various metal ions, anions and carbon sources, which are easily available from plants, coal, fossil fuels, and natural gases. Thus, they are accessible from both economic and environmental perspectives such as ecological footprint, pollution, and water usage purity. Also, their synthesis consumes less energy ranging from different manufacturing processes to disposal, highlighting renewable energy alternatives. Also, the waste generated as a by-product should be minimized and the impact of their disposal on the environment investigated. Otherwise, by reprocessing and reusability of these materials must drastically reduce the environmental footprint and be economically feasible. Finally, given that they are non-hazardous materials, they can be disposed as solid waste.

### 6.2 Challenges and future perspectives

According to demography, global warming and the extinction of fossil fuels have increased across the globe, and there is a long-standing demand for sustainable, harmless, and environmentally friendly green energy for the future generation. The improvement of future research guided by experimental

Table 4 Summary of the literature survey discussed in this review including the results of electrochemical applications from various LDH/CNT heterostructure composites

| S. no. | Electrode materials | Synthesis route | Specific capacitance ($F\ g^{-1}$) | Energy density ($W\ h\ kg^{-1}$) | Power density ($W\ kg^{-1}$) | Capacitance retention (%) | Ref. |
|---|---|---|---|---|---|---|---|
| 1 | CoAl LDH/CNT, CoAl LDH/g-$C_3N_4$, CoAl LDH/AC, | Hydrothermal | 1891 for CoAl LDH/AC | — | — | 66.3 | 2 |
| 2 | CoAl LDH/CNT/CNH | Hydrothermal | 754 | 62.2 | 632.5 | 78.5 | 72 |
| 3 | CoAl LDH/CNT | Hydrothermal | 884 | 28 | 444.1 | 88 | 73 |
| 4 | NiCo LDH/N-CNT | Hydrothermal | 693 C $g^{-1}$ | 51.3 | 533 | 80 | 58 |
| 5 | NiCo LDH/MX- MWCNT | Hydrothermal | 1382.2 C $g^{-1}$ | 78.7 ± 0.8 | 800 | 96.7 | 59 |
| 6 | CoNiFe(SDS)–LDH/CNFs/, CoNiFe(SDS)–LDH/CNT, CoNiFe(SDS)–LDH/CB | Hydrothermal | 176.33 of CoNiFe (SDS)–LDH/CNT | 43.0 | 779.9 | 85.2 | 62 |
| 7 | CoNiFe LDH/CNT//AC | Hydrothermal | 96.1 | 29.9 | 750.5 | 85 | 63 |
| 8 | NiAl LDH/CNTs | Hydrothermal | 694 | — | — | 87 | 74 |
| 9 | NiAl LDH/CNT | Hydrothermal | 1017 C $g^{-1}$ | — | — | 85 | 64 |
| 10 | NiFe LDH/CNT, AC//LDH–RGO–CNFs | Hydrothermal | 1330.2 of AC// LDH–RGO–CNFs | 33.7 | 785.8 | 97.1 | 75 |
| 11 | NiCoCe LDH/CNT | Hydrothermal | 187.2 | — | — | 85.6 | 7 |
| 12 | NiCo LDH/CNTs | Hydrothermal | 1628 | 38.89 | 800 | 99.379 | 60 |
| 13 | NiAl LDH/CNT/cellulose | Hydrothermal | 72.4 | 32.6 | 18 000 | 99 | 65 |
| 14 | NiAl LDH/CNT | Electrodeposition | 1800 | 35.6 | 7531.9 | 65.8 | 87 |
| 15 | rGO–FeO–CNT-700–NiFe LDH | Electrodeposition | 411.9 | 41.4 | 5600 | 102.2 | 66 |
| 16 | NiCo LDH/CNT | Electrodeposition | 758 C $g^{-1}$ | 26.2 | 7569.2 | 112.5 | 88 |
| 17 | NiCo LDH/CNTs | Electrodeposition | 176.33 mA h $g^{-1}$ | 37.38 | 800 | 90.22 | 89 |
| 18 | NiGa LDH/CNT//CC | Electrodeposition | 2580 | 52 | 952 | 83.3 | 67 |
| 19 | NiAl LDH/CNT | Co-precipitation | 2447 | — | — | 90.1 | 78 |
| 20 | NiCo LDH/CNT@CoS | Co-precipitation | 2794.6 | 31.38 | 3750 | 87 | 79 |
| 21 | NiMn LDH/CNTs/rGO | Co-precipitation | 1268 | — | — | — | 80 |
| 22 | NiMn LDH/CNT | Co-precipitation | 2960 | 88.3 | 850 | 79.5 | 68 |
| 23 | NiAl LDH/CNT | Reflux | 1500 | 52 | — | 70.3 | 83 |
| 24 | NiCo LDH@$Co_3O_4$/CNT | Reflux | 744 C $g^{-1}$ | 58.3 | 575 | 90 | 61 |
| 25 | NiCoAl LDH/CNT/rGO | Reflux | 1188 | — | — | 72 | 70 |
| 26 | NiV LDH/CNT | Reflux | 1493 | 95.6 | 5417.8 | 68.8 | 69 |
| 27 | NiAl LDH/CNT/rGO | Solvothermal | 1562 | — | — | — | 57 |
| 28 | NiCo LDH/CNT | Chemical deposition | 1843 | 51 | 3300 | — | 93 |
| 29 | NiCo LDH/CNT/NF | Thermal chemical vapour deposition (TCVD) | 2046 | 41.7 | 8700 | 78 | 98 |

designs can be achieved by addressing some key points, which will be useful information with the minimum number of experiments. (1) Hybrid supercapacitor system design: experiments with hybrid systems that integrate supercapacitors with batteries (*e.g.*, lithium-ion) to assess performance metrics such as energy density and cycle life. (2) Material synthesis variations: synthesize various carbon-based materials using different methods (*e.g.*, hydrothermal, sol–gel) to study the impact on specific surface area and pore size distribution. (3) Electrochemical impedance spectroscopy (EIS): EIS over a wide frequency range to assess the charge transfer resistance, ionic diffusion, and dielectric properties of materials. (4) Data interpretation: a machine learning approach or advanced statistical data may provide deeper insights. In fact, it will also benefit consistency or modification requirements, leading to a new skillful representation model with variation of analysis. (4) Refinement of objectives: a specific goal must be defined with proposed experimental design. Among the EES devices, SCs are the most inevitable and emerging candidate to fulfill all the demands in the energy storage field with minimal loss in an extended range of parameters variation in terms of charge–discharge, specific capacitance, capacitance retention rate, and cycle stability, but their only limitation is their low energy density in comparison to batteries and fuel cells. Therefore, efficient, permanent, and calculated technology will be vital to avoid this hurdle. The factors in detail are discussed below in Fig. 18.

- Technology improvement of energy density: presently, technology-based research is on-going to improve the development process of LDH/CNT nanocomposite electrodes and achieve the best energy density output, but it is long way forward, with difficulties in finding electrolytes with higher correlated electrochemical values. Also, this can be achieved by only increasing specific surface area and operating window potential.
- Commercial brand: the healthy development of supercapacitors will never be neglected from international or national standards with a reasonable market price. Therefore their storage, precautions, standard operating procedures, performance test methods, electrolyte specification, production technical report, and green recycling disposal should be labeled.
- Assembly with electrical components: supercapacitors are often used in conjunction with regenerative braking systems. Ensuring the compatibility and household or industrial optimal operation between these systems is critical but complex.
- Control systems: the system design is complex for the development of sophisticated control algorithms to manage the interplay between supercapacitors and batteries.

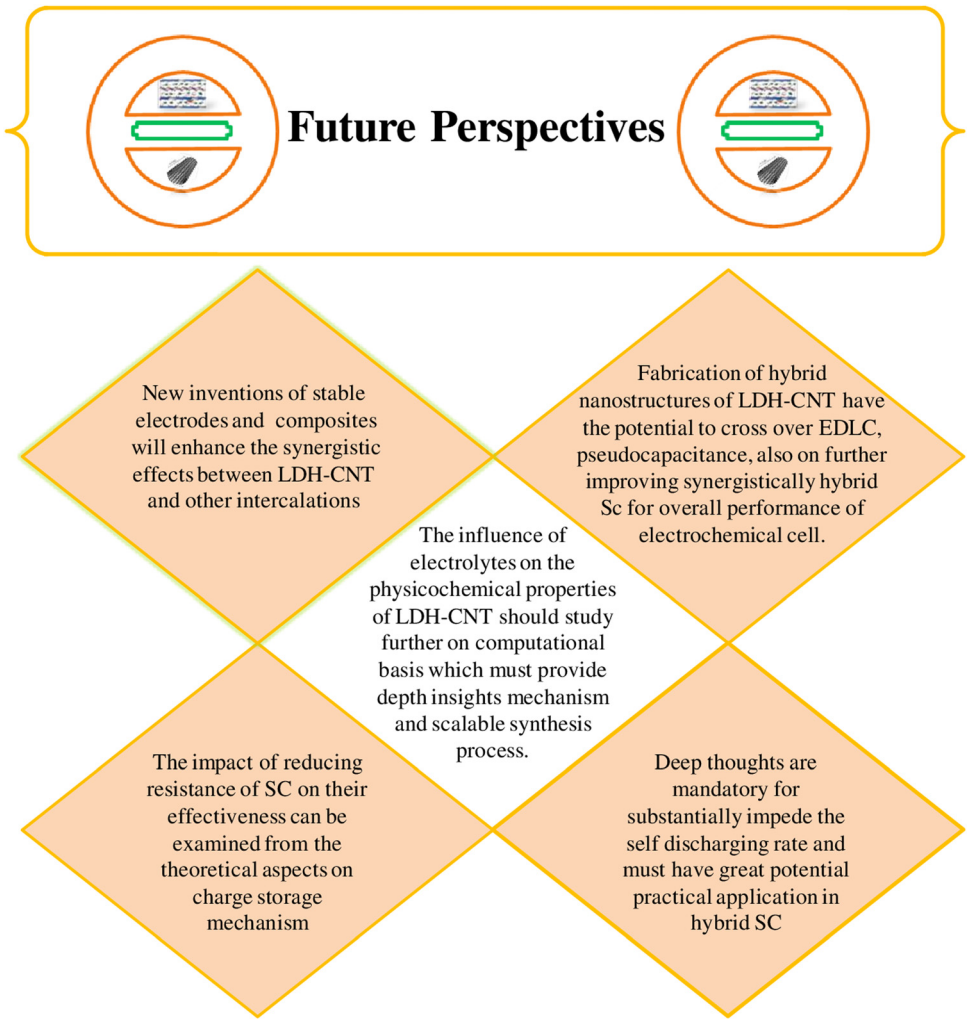


Fig. 18 Gist of future perspectives.

• Stable electrodes: the invention and fabrication of new binary/ternary LDHs combined with CNT is a challenging topic, requiring a sufficient nano pore distribution of maximum specific surface area for faradaic reversible redox reaction active sites to create diffused electrons/ions. Also, these mobile charge particles will further enhance the activities of SCs with suitable dopants without altering the phase of the composite.

• Aqueous or non-aqueous electrolyte: analysis of both the electrode and electrolyte is crucial for EES devices, especially SCs, which are being treated as efficient and the most advanced energy storage devices to execute all needs. A reduction in the diffusion length of ions in the electrolyte is beneficial for fast transport to the collector current *via* a stable electrode, resulting in a better performance for electrochemical reactions as well as high energy/power per unit volume.

• Resistance of SC devices: reducing the resistance of the whole system, including the ESR (equivalent series resistance) and charge transfer resistance, is a significant hurdle to overcome and achieve the best output during a chemical reaction. This arises due to the quantity of materials/composites used in ultracapacitors, which resist the path of charged particles. Hence, the use of suitable conductive materials as the electrolyte is the only solution for minimizing the specific capacitance loss, leading to fast charging/discharging, high retention rate, and high energy and power density.

• Minimizing self-discharge: SCs have a conventional self-charging process through electron/ion transfer from the electrolyte into the electrode for charge storage by changing the potential according to the Nernst equation. The material defect, charge distribution at the faradaic sites, and internal resistance often generate leakage currents, which significantly govern the intrinsic self-discharge and are the only major disadvantages of SC. The second reason is that water formation by oxygen reduction at the two electrodes causes unwanted self-discharge and a short lifetime. In practical aspects, groundbreaking research on proton exchange separators can eliminate the self-discharging process unconditionally through proton transfer from the LDH/CNT anode to the LDH/CNT cathode. Despite the many efforts to tackle the issue of major drawbacks, (1) low energy density and (2) self-discharging are concerns in a methodological calculation for researchers to build new LDH/CNT hybrid composites. These are the only distinguished

materials that possess all the properties of SCs and other EESDs.

The power density, specific capacitance, capacitance retention, and stability of composites have always shown impressive results in electrochemical studies. However, there are gaps in finding optimized data by doping/modifying the structure to further enhance the kinetic balance of LDH/CNT-based hybrid SCs, which is discussed below.

(1) Incorporation of proper element: doping suitable elements in the lattice site of composites without any defects will enhance their electrical conductivity, leading to fast electron/ion transfer and charging/discharging. Therefore, the search for new elements must be innovative to bring outstanding output in LDH/CNT and their prospects for application in SCs. Also, the faradaic reversible redox reaction benefits from tunable structures, ultra-nanopores for maximum surface area, large active sides, and conductive electrolyte due to energetic ions/electrons, which will exhibit excellent performances in integrated composites.

(2) Interaction between LDH and CNT: there must be a clear understanding of the interactions between LDH and CNT, *i.e.*, van der Waals force, weak force, and covalent bonds in different layers, which will help improve the electrochemical performances of LDH/CNT hybrid composite-based SCs.

(3) Proton exchange separator: the partial redox reaction, current leakage, faradaic reaction, and charge distribution promote inherent self-discharging. Thus, a proton exchange separator can be employed to restrict the self-discharging process and act as a barrier for protons at the anode, but is suppressed to the cathode by minimizing the faradaic reaction at electrodes and the discharge rate.

(4) Cost effective: the synthesis of LDH/CNT hybrid electrodes is much cheaper than other composites using any technique, safe, eco-friendly, requires less energy, and no harmful gas is produced.

## 7. Conclusion

In this review, we elaborated on the fundamental storage mechanism, its advantages and drawbacks, different types of synthesis methods, and outcomes of varying the incorporated transition metal in binary/ternary LDH integrated with CNT to form nanohybrids to deliver high energy and power density, better specific capacitance and retention rate for application in flexible, wearable, and stable long-life EES device ultracapacitors. A detailed analysis of LDH/CNT composites and their inherent effects in diverse applications on the electrochemical study of storage devices and the intrinsic effect mechanism with bio-sustainability were presented to cover an extensive chapter on nanohybrid composite-based EES devices. Furthermore, the electrochemical properties and updated advancement of LDH/CNT nanocomposites were analyzed, including systematic experiments and high-resolution characterization (XRD, HRTEM, FESEM, XPS, Raman spectroscopy, and electrochemical workstation) with varying parameters and conditions, but still there is much room to be filled regarding greater accuracy, which will be challenging and encouraging.

The collective knowledge of LDH/CNT nanocomposites synthesized by different techniques was terrific. The awareness in this field has increased due to their extraordinary properties, which were discussed in this review. The importance of these compounds created a milestone in energy storage and a remarkable achievement among supercapacitor enthusiasts. All their features and properties were characterized by high-end equipment (both analytical and microscopy), which motivates further improvement in detail, analyzing both internal and external morphology and electrochemical reaction setup. However, there are mixed results in different synthesis methods regarding specific capacitance, energy and power density, retention rate, and cycle stability, considering the different surface areas, tunable structures, and electrical/thermal conductivity of electrodes and their strength. Therefore, the broad operando research on LDH/CNT-based electrodes keeps the door open across the globe for its magical electrochemical properties as a hybrid supercapacitor. Although EDLC and pseudocapacitors play a role in many applications, they are limited to some extent in wide applications and many more. Accordingly, nanohybrid supercapacitors based on the fusion of layered double hydroxides and carbon nanotubes have essential aspects in the field of hybrid energy in different computer storage chips, vehicles, cars, and other storage devices given that they overcome all the barriers associated with their EDLC and pseudocapacitor contemporaries. Also, it is essential for continuous research to invent worthwhile methods to fabricate LDH/CNT nanocomposite electrode-based hybrid supercapacitors to explore and develop new energy generation and storage technologies, which can overtake all the results for the commercially available devices with great potential in future endeavors.

## Declaration of generative AI in scientific writing

The authors now declare that there is no use of AI-related tools or software to analyze and prepare this manuscript.

## Data availability

Data will be made available on request.

## Conflicts of interest

There is no competing financial interest or any beneficial purpose.

## Acknowledgements

The authors are thankful to Siksha 'O' Anusandhan (Deemed to be University) management for their constant support and motivation.

## References


1 P. Deb Shuvra and S. McNamara, *AIP Adv.*, 2014, **4**, 127158, DOI: 10.1063/1.4905460.

2 Z. Yong, S. Xue, X. Yan, H. Gao and K. Gao, Preparation and electrochemical properties of cobalt aluminum layered double hydroxide/carbon-based integrated composite electrode materials for supercapacitors, *Electrochim. Acta*, 2023, **442**, 141822, DOI: 10.1016/j.electacta.2023.141822.

3 T. Shweta, A. Arya, A. Gaur and A. L. Sharma, Transition metal dichalcogenide (TMDs) electrodes for supercapacitors: a comprehensive review, *J. Condens. Matter Phys.*, 2021, **33**, 303002, DOI: 10.1088/1361-648X/abfb3c.

4 V. G. B. Bidita and V. O. Nyamori, Layered double hydroxide-and graphene-based hierarchical nanocomposites: Synthetic strategies and promising energy conversion and conservation applications, *Nano Res.*, 2016, **9**, 3598–3621.

5 A. Ravikant, M. Sharma, S. Sharma, A. Kumar, G. Malik, R. Boukherroub and R. Chandra, Metal nitrides as efficient electrode material for supercapacitors: A review, *J. Energy Storage*, 2022, **56**, 105912, DOI: 10.1016/j.est.2022.105912.

6 S. Jinfeng, C. Liu, X. Song, J. Zhang, Y. Liu, L. Liang, R. Jiang and C. Yuan, Electrochemical energy storage devices under particular service environments: Achievements, challenges, and perspective, *Appl. Phys. Rev.*, 2022, **9**, 031301, DOI: 10.1063/5.0086130.

7 D. Mohammad, H. Allami and M. M. Momeni, Construction of Ce-doped NiCo-LDH@CNT nanocomposite electrodes for high-performance supercapacitor application, *Energy Fuels*, 2020, **35**, 1831–1841, DOI: 10.1021/acs.energyfuels.0c03764.

8 Z. S. Iro, C. Subramani and S. S. Dash, A brief review on electrode materials for supercapacitor, *Int. J. Electrochem. Sci.*, 2016, **11**, 10628–10643, DOI: 10.20964/2016.12.50.

9 S. Fleischmann, J. B. Mitchell, R. Wang, C. Zhan, D. Jiang, V. Presser and V. Augustyn, Pseudocapacitance: from fundamental understanding to high power energy storage materials, *Chem. Rev.*, 2020, **14**, 6738–6782, DOI: 10.1021/acs.chemrev.0c00170.

10 K. S. Kumar, N. Choudhary, Y. Jung and J. Thomas, Recent advances in two-dimensional nanomaterials for supercapacitor electrode applications, *ACS Energy Lett.*, 2018, **2**, 482–495, DOI: 10.1021/acsenergylett.7b01169.

11 H. Sheng, L. Jiang, Q. Wang, Z. Zhang, Y. Lv, H. Ma, H. Bi, J. Yuan, M. Shao, F. Li and W. Li, A soft implantable energy supply system that integrates wireless charging and biodegradable Zn-ion hybrid supercapacitors, *Sci. Adv.*, 2023, **46**, eadh8083, DOI: 10.1126/sciadv.adh8083.

12 S. Tanwar and A. L. Sharma, Insight into the use of biopolymer in hybrid electrode materials for supercapacitor applications—A critical review, *J. Appl. Phys.*, 2023, **18**, 180701, DOI: 10.1063/5.0138950.

13 G. G. Prasad, N. Shetty, S. Thakur, Rakshitha and K. B. Bommegowda, Supercapacitor technology and its applications: a review, *IOP Conf. Ser.:Mater. Sci. Eng.*, 2019, **561**, 012105, DOI: 10.1088/1757-899X/561/1/012105.

14 L. L. Zhang and X. S. Zhao, Carbon-based materials as supercapacitor electrodes, *Chem. Soc. Rev.*, 2019, **38**, 2520–2531, DOI: 10.1039/B813846J.

15 A. L. M. Reddy, S. R. Gowda, M. M. Shaijumon and P. M. Ajayan, Hybrid nanostructures for energy storage applications, *Adv. Mater.*, 2012, **37**, 5045–5064, DOI: 10.1002/adma.201104502.

16 A. Muzaffar, M. B. Ahamed, K. Deshmukh and J. Thirumalai, A review on recent advances in hybrid supercapacitors: Design, fabrication and applications, *Renewable Sustainable Energy Rev.*, 2019, **101**, 123–145, DOI: 10.1016/j.rser.2018.10.026.

17 P. Zaccagnini and A. Lamberti, A perspective on laser-induced graphene for micro-supercapacitor application, *Appl. Phys. Lett.*, 2022, **120**, 100501, DOI: 10.1063/5.0078707.

18 S. Huang, X. Zhu, S. Sarkar and Y. Zhao, Challenges and opportunities for supercapacitors, *APL Mater.*, 2019, **7**, 100901, DOI: 10.1063/1.5116146.

19 J. Castro-Gutiérrez, A. Celzard and V. Fierro, Energy storage in supercapacitors: Focus on tannin-derived carbon electrodes, *Front. Mater.*, 2020, **7**, 217, DOI: 10.3389/fmats.2020.00217.

20 T. Yu, S. Li, F. Li, L. Zhang, Y. Wang and J. Sun, *In situ* synthesized and induced vertical growth of cobalt vanadium layered double hydroxide on few-layered V2CTx MXene for high energy density supercapacitors, *J. Colloid Interface Sci.*, 2024, **661**, 460–471, DOI: 10.1016/j.jcis.2024.01.206.

21 S. Kulandaivalu, N. H. N. Azman and Y. Sulaiman, Advances in layered double hydroxide/carbon nanocomposites containing $Ni^{2+}$ and $Co^{2+/3+}$ for supercapacitors, *Front. Mater. Sci.*, 2020, **7**, 147, DOI: 10.3389/fmats.2020.00147.

22 T. Yu, S. Li, L. Zhang, F. Li, J. Wang, H. Pan and D. Zhang, In situ growth of ZIF-67- derived nickel-cobalt-manganese hydroxides on 2D V2CTx MXene for dual-functional orientation as high-performance asymmetric supercapacitor and electrochemical hydroquinone sensor, *J. Colloid Interface Sci.*, 2023, **629**, 546–558, DOI: 10.1016/j.jcis.2022.09.107.

23 Y. Zhang, X. Jing, X. H. Yan, H. L. Gao, K. Z. Gao, Y. Cao, S. Hu and Y. Y. Zhang, Rational design of NiMn-based electrode materials for high-performance supercapacitors, *Coord. Chem. Rev.*, 2024, **499**, 215494, DOI: 10.1016/j.ccr.2023.215494.

24 Y. Zhang, Y. Y. Zhang, C. E. Li, X. H. Yan, S. Hu, R. B. Yin, Y. F. Wei, K. Z. Gao and H. L. Gao, Research progress of $NiFe_2O_4$ electrode materials in supercapacitors: Preparation, modification, structural regulation, and future challenges, *Coord. Chem. Rev.*, 2024, **519**, 216103, DOI: 10.1016/j.ccr.2024.216103.

25 Y. Zhang, S. C. Xue, X. H. Yan, H. L. Gao and K. Z. Gao, Preparation and electrochemical properties of cobalt aluminum layered double hydroxide/carbon-based integrated composite electrode materials for supercapacitors, *Electrochim. Acta*, 2023, **442**, 141822, DOI: 10.1016/j.electacta.2023.141822.

26 Y. Zhang, C. G. Zhou, X. H. Yan, Y. Cao, H. L. Gao, H. W. Luo, K. Z. Gao, S. C. Xue and X. Jing, Recent advances and perspectives on graphene-based gels for superior flexible all-solid-state supercapacitors, *J. Power Sources*, 2023, **565**, 232916, DOI: **10.1016/j.jpowsour.2023.232916**.

27 P. Nakhanivej, H. H. Rana, H. Kim, B. Y. Xia and H. S. Park, Transport and durability of energy storage materials operating at high temperatures, *ACS Nano*, 2020, **14**, 7696–7703, DOI: **10.1021/acsnano.0c04402**.

28 X. Y. Luo, Y. Chen and Y. Mo, A review of charge storage in porous carbon-based supercapacitors, *New Carbon Mater.*, 2021, **36**, 49–68, DOI: **10.1016/S1872-5805(21)60004-5**.

29 T. Chen and L. Dai, Carbon nanomaterials for high-performance supercapacitors, *Mater. Today*, 2013, **16**, 272–280, DOI: **10.1016/j.mattod.2013.07.002**.

30 G. Z. Chen, Linear and non-linear pseudocapacitances with or without diffusion control, *Prog. Nat. Sci.:Mater.*, 2021, **31**, 792–800, DOI: **10.1016/j.pnsc.2021.10.011**.

31 A. Gomes, D. Cocke, D. Tran and A. Baksi, *Layered double hydroxides in energy research: advantages and challenges, Energy Technology 2015: Carbon Dioxide Management and Other Technologies*, 2015, pp. 309–316, **https://link.springer.com/chapter/10.1007/978-3-319-48220-0_34**.

32 A. Bhat, S. Anwer, K. S. Bhat, M. I. Mohideen, K. Liao and A. Qurashi, Prospects challenges and stability of 2D MXenes for clean energy conversion and storage applications, *npj 2D Mater. Appl.*, 2021, 61.

33 P. Sun, R. Ma, X. Bai, K. Wang, H. Zhu and T. Sasaki, Single-layer nanosheets with exceptionally high and anisotropic hydroxyl ion conductivity, *Sci. Adv.*, 2017, **3**, e1602629, DOI: **10.1126/sciadv.1602629**.

34 P. K. Ray, P. Mohanty and K. Parida, Recent advancements of NiCo LDH and graphene based nanohybrids for supercapacitor application, *J. Energy Storage*, 2023, **72**, 108335, DOI: **10.1016/j.est.2023.108335**.

35 F. Bonaccorso, L. Colombo, G. Yu, M. Stoller, V. Tozzini, A. C. Ferrari, R. S. Ruoff and V. Pellegrini, Graphene related two-dimensional crystals, and hybrid systems for energy conversion and storage, *Science*, 2015, **347**, 1246501, DOI: **10.1126/science.1246501**.

36 L. W. Le Fevre, A. Ejigu, R. Todd, A. J. Forsyth and R. A. Dryfe, High temperature supercapacitors using water-in-salt electrolytes: stability above 100 °C, *Chem. Commun.*, 2021, **57**, 5294–5297, DOI: **10.1039/D1CC01087E**.

37 T. Dey, A. Dial, P. R. Corridon and S. Dutta, Biosupercapacitors with minimized Self-Discharge, *J. Chem. Eng.*, 2023, **470**, 144101, DOI: **10.1016/j.cej.2023.144101**.

38 J. Zhao and A. F. Burke, Review on supercapacitors: Technologies and performance evaluation, *J. Energy Chem.*, 2021, **59**, 276–291, DOI: **10.1016/j.jechem.2020.11.013**.

39 H. W. Park and K. C. Roh, Recent advances in and perspectives on pseudocapacitive materials for supercapacitors–a review, *J. Power Sources*, 2023, **557**, 232558, DOI: **10.1016/j.jpowsour.2022.232558**.

40 K. K. Kar, *Handbook of nanocomposite supercapacitor materials II*, Springer International Publishing, Cham, 2020, vol. 302, **https://link.springer.com/book/10.1007/978-3-030-52359-6**.

41 P. Priyadarshini and K. Parida, Two-dimensional metal-organic frameworks and their derived materials: Properties, synthesis and application in supercapacitors field, *J. Energy Storage*, 2024, **87**, 111379, DOI: **10.1016/j.est.2024.111379**.

42 S. Nayak and K. Parida, Superactive NiFe-LDH/graphene nanocomposites as competent catalysts for water splitting reactions, *Inorg. Chem. Front.*, 2020, **7**, 3805–3836, DOI: **10.1039/D0QI00700E**.

43 S. Nayak and K. Parida, Dynamics of charge-transfer behavior in a plasmon-induced quasi-type-II p–n/n–n dual heterojunction in Ag@$Ag_3PO_4$/g-$C_3N_4$/NiFe LDH nanocomposites for photocatalytic Cr(VI) reduction and phenol oxidation, *ACS Omega*, 2023, **7**, 7324–7343.

44 A. Mohanty, D. Jaihindh, Y. P. Fu, S. P. Senanayak, L. S. Mende and A. Ramadoss, An extensive review on three dimension architectural Metal-Organic Frameworks towards supercapacitor application, *J. Power Sources*, 2021, **488**, 229444, DOI: **10.1016/j.jpowsour.2020.229444**.

45 T. S. Mathis, N. Kurra, X. Wang, D. Pinto, P. Simon and Y. Gogotsi, Energy storage data reporting in perspective—guidelines for interpreting the performance of electrochemical energy storage systems, *Adv. Energy Mater.*, 2019, **9**, 1902007, DOI: **10.1002/aenm.201902007**.

46 A. Nanwani, K. A. Deshmukh, P. Sivaraman, D. R. Peshwe, I. Sharma, S. J. Dhoble, H. C. Swart, A. D. Deshmuk and B. K. Gupta, Two-dimensional layered magnesium–cobalt hydroxide crochet structure for high rate and long stable supercapacitor application, *npj 2D Mater. Appl.*, 2019, 45.

47 U. S. Nur, K. K. Ying and N. I. Khuan, *Electrodeposition: Principles, Applications and Methods*, 2021.

48 M. Mazloum-nArdakani, H. Mohammadian-Sarcheshmeh, H. Naderi, F. Farbod and F. Sabaghian, Fabrication of a high-performance hybrid supercapacitor using a modified graphene aerogel/cerium oxide nanoparticle composite, *J. Energy Storage*, 2019, **26**, 100998, DOI: **10.1016/j.est.2019.100998**.

49 X. Li, D. Du, Y. Zhang, W. Xing, Q. Xue and Z. Yan, Layered double hydroxides toward high-performance supercapacitors, *J. Mater. Chem. A*, 2017, **5**, 15460–15485, DOI: **10.1039/C7TA04001F**.

50 M. Laipan, J. Yu, R. Zhu, J. Zhu, A. T. Smith, H. He, D. O'Hare and L. Sun, Functionalized layered double hydroxides for innovative applications, *Mater. Horiz.*, 2020, **7**, 715–745, DOI: **10.1039/C9MH01494B**.

51 L. Guan, L. Yu and G. Z. Chen, Capacitive and non-capacitive faradaic charge storage, *Electrochim. Acta*, 2016, **206**, 464–478, DOI: **10.1016/j.electacta.2016.01.213**.

52 A. J. Khan, M. Hanif, M. S. Javed, S. Hussain, W. Zhong, M. Saleem and Z. Liu, Energy storage properties of hydrothermally processed, nanostructured, porous $CeO_2$ nanoparticles, *J. Electroanal. Chem.*, 2020, **865**, 114158, DOI: **10.1016/j.jelechem.2020.114158**.

53 J. Jiang, X. Huang, R. Sun, X. Chen and S. Han, Interface engineered hydrangea-like $ZnCo_2O_4$/NiCoGa-layered double

hydroxide@ polypyrrole core-shell heterostructure for high-performance hybrid supercapacitor, *J. Colloid Interface Sci.*, 2023, **640**, 662–679, DOI: **10.1016/j.jcis.2023.02.132**.

54 L. Kong, M. Cheng, H. Huang, J. Pang, S. Liu, Y. Xu and X. H. Bu, Metal-organic frameworks for advanced aqueous ion batteries and supercapacitors, *EnergyChem*, 2022, **4**, 100090, DOI: **10.1016/j.enchem.2022.100090**.

55 T. Chen, S. Wei and Z. Wang, $NiCo_2S_4$-based composite materials for supercapacitors, *ChemPlusChem*, 2020, **85**, 43–56, DOI: **10.1002/cplu.201900288**.

56 X. He and X. Zhang, A comprehensive review of supercapacitors: Properties, electrodes, electrolytes and thermal management systems based on phase change materials, *J. Energy Storage*, 2022, **56**, 106023, DOI: **10.1016/j.est.2022.106023**.

57 W. Yang, Z. Gao, J. Wang, J. Ma, M. Zhang and L. Liu, Solvothermal one-step synthesis of Ni–Al layered double hydroxide/carbon nanotube/reduced graphene oxide sheet ternary nanocomposite with ultrahigh capacitance for supercapacitors, *ACS Appl. Mater. Interfaces*, 2013, **5**, 5443–5454, DOI: **10.1021/am4003843**.

58 R. Liu, Y. Wang, S. Sun, C. Chen and X. Wu, CoNi layered double hydroxide anchored on N-doped carbon coated carbon nanotubes network with 3D Core-shell structure for all-solid-state supercapacitors, *J. Electroanal. Chem.*, 2020, **878**, 114571, DOI: **10.1016/j.jelechem.2020.114571**.

59 Q. Ma, Y. Wang, X. Han, Y. Zhang and W. He, Integrated novel carbon materials/layered double metal hydroxides component and function towards enhanced electrochemical performance of supercapacitor, *Electrochim. Acta*, 2022, **435**, 141367, DOI: **10.1016/j.electacta.2022.141367**.

60 M. Huang, Y. Wang, J. Chen, D. He, J. He and Y. Wang, Biomimetic design of NiCo LDH composites linked by carbon nanotubes with plant conduction tissues characteristic for hybrid supercapacitors, *Electrochim. Acta*, 2021, **381**, 138289, DOI: **10.1016/j.electacta.2021.138289**.

61 D. Wei, Y. Zhang, X. Zhu, M. Fan and Y. Wang, CNT/$Co_3S_4$@ NiCo LDH ternary nanocomposites as battery-type electrode materials for hybrid supercapacitors, *J. Alloys Compd.*, 2020, **824**, 153937, DOI: **10.1016/j.jallcom.2020.153937**.

62 Q. Ding, J. Li, S. Li, J. Wang, W. Huang, S. Sun, Y. Xu and H. Li, Preparation of novel composites based on SDS intercalated CoNiFe–LDH and carbon materials for advanced asymmetric supercapacitors, *J. Energy Storage*, 2023, **67**, 107556, DOI: **10.1016/j.est.2023.107556**.

63 J. Wang, Q. Ding, C. Bai, F. Wang, S. Sun, Y. Xu and H. Li, Synthesis of CNTs/CoNiFe-LDH nanocomposite with high specific surface area for asymmetric supercapacitor, *Nanomaterials*, 2021, **11**, 2155, DOI: **10.3390/nano11092155**.

64 Y. Wang, Z. Chen, H. Li, J. Zhang, X. Yan, K. Jiang, D. Den Engelsen, L. Ni and D. Xiang, The synthesis and electrochemical performance of core-shell structured Ni-Al layered double hydroxide/carbon nanotubes composites, *Electrochim. Acta*, 2016, **222**, 185–193, DOI: **10.1016/j.electacta.2016.09.073**.

65 S. Acharya, S. De and G. C. Nayak, CNT/LDH-stabilized biomass-derived nanocellulose as a low-cost alternative for asymmetric supercapacitors: Impact of sources of nanocellulose, *ACS Appl. Mater. Interfaces*, 2023, **5**, 406–417, DOI: **10.1021/acsaelm.2c01440**.

66 C. Hsiao, C. Lee and N. Tai, High retention supercapacitors using carbon nanomaterials/iron oxide/nickel-iron layered double hydroxides as electrodes, *J. Energy Storage*, 2022, **46**, 103805, DOI: **10.1016/j.est.2021.103805**.

67 C. Li, G. Zhang, X. Li, H. Wang, P. Huo, Y. Yan and X. Wang, Construction of hierarchical layered hydroxide grown *in situ* on carbon tubes derived from a metal–organic framework for asymmetric supercapacitors, *Dalton Trans.*, 2021, **50**, 7337, DOI: **10.1039/D1DT00916H**.

68 J. Zhao, J. Chen, S. Xu, M. Shao, Q. Zhang, F. Wei, J. Ma, M. Wei, D. G. Evans and X. Duan, Hierarchical NiMn layered double hydroxide/carbon nanotubes architecture with superb energy density for flexible supercapacitors, *Adv. Funct. Mater.*, 2014, **24**, 2938–2946, DOI: **10.1002/adfm.201303638**.

69 Q. Tu, J. Zhang, S. Cai, K. Zhang, H. Zhan, S. Huang, L. Chen and X. Sun, One-step preparation of NiV-LDH@ CNT hierarchical composite for advanced asymmetrical supercapacitor, *Adv. Eng. Mater.*, 2022, **24**, 2101174, DOI: **10.1002/adem.202101174**.

70 C. Yu, J. Yang, C. Zhao, X. Fan, G. Wang and J. Qiu, Nanohybrids from NiCoAl-LDH coupled with carbon for pseudocapacitors: understanding the role of nanostructured carbon, *Nanoscale*, 2014, **6**, 3097–3104, DOI: **10.1039/C3NR05477B**.

71 A. B. Djurisic, X. Y. Chen and Y. H. Leung, Recent progress in hydrothermal synthesis of zinc oxide nanomaterials, *Recent Pat. Nanotechnol.*, 2012, **6**, 124, DOI: **10.2174/187221012800270180**.

72 G. Yang, T. Takei, Y. Zhu, E. Iranmanesh, B. Liu, Z. Li, J. Wang, P. Hiralal, G. A. Amaratunga, O. Fontaine and H. Zhou, Constructing an efficient conductive network with carbon-based additives in metal hydroxide electrode for high-performance hybrid supercapacitor, *Electrochim. Acta*, 2021, **397**, 139242, DOI: **10.1016/j.electacta.2021.139242**.

73 L. Yu, N. Shi, Q. Liu, J. Wang, B. Yang, B. Wang, H. Yan, Y. Sun and X. Jing, Facile synthesis of exfoliated Co–Al LDH–carbon nanotube composites with high performance as supercapacitor electrodes, *Phys. Chem. Chem. Phys.*, 2014, **16**, 17936–17942, DOI: **10.1039/C4CP02020K**.

74 C. Bai, S. Sun, Y. Xu, R. Yu and H. Li, Facile one-step synthesis of nanocomposite based on carbon nanotubes and Nickel-Aluminum layered double hydroxides with high cycling stability for supercapacitors, *J. Colloid Interface Sci.*, 2016, **480**, 57–62, DOI: **10.1016/j.jcis.2016.07.001**.

75 F. Wang, T. Wang, S. Sun, Y. Xu, R. Yu and H. Li, One-step synthesis of Nickle Iron-layered double hydroxide/reduced graphene oxide/carbon nanofibres composite as electrode materials for asymmetric supercapacitor, *Sci. Rep.*, 2018, **8**, 8908, DOI: **10.1038/s41598-018-27171-0**.

76 T. Ahn, J. H. Kim, H. M. Yang, J. W. Lee and J. D. Kim, Formation pathways of magnetite nanoparticles by coprecipitation method, *J. Phys. Chem. C*, 2012, **116**, 6069–6076, DOI: 10.1021/jp211843g.

77 I. F. Cruz, C. Freire, J. P. Araújo, C. Pereira and A. M. Pereira, Multifunctional ferrite nanoparticles: from current trends toward the future, *Magnetic nanostructured materials*, 2018, vol. 59, pp. 59–116, DOI: 10.1016/B978-0-12-813904-2.00003-6.

78 K. Luo, J. Zhang, W. Chu and H. Chen, Facile fabrication of nickel aluminum layered double hydroxide/carbon nanotube electrodes toward high-performance supercapacitors, *ACS Omega*, 2020, **5**, 24693–24699, DOI: 10.1021/acsomega.0c03283.

79 X. Yue, Z. Chen, C. Xiao, G. Song, S. Zhang and H. He, Synthesis of CNT@CoS/NiCo layered double hydroxides with hollow nanocages to enhance supercapacitors performance, *Nanomaterials*, 2022, **12**, 3509, DOI: 10.3390/nano12193509.

80 M. Li, F. Liu, X. B. Zhang and J. P. Cheng, A comparative study of Ni–Mn layered double hydroxide/carbon composites with different morphologies for supercapacitors, *Phys. Chem. Chem. Phys.*, 2016, **18**, 30068, DOI: 10.1039/C6CP05119G.

81 H. Deng, J. Liu, T. Yang and S. Wu, Numerical study and visualization on flow characteristics of reflux condensation in air-cooled condenser, *Appl. Therm. Eng.*, 2019, **148**, 1310, DOI: 10.1016/j.applthermaleng.2018.11.109.

82 N. P. Raju, D. Tripathi, S. Lahiri and R. Thangavel, Heat reflux sonochemical synthesis of $Cu_3BiS_3$ quantum dots: Experimental and first-principles investigation of spin–orbit coupling on structural, electronic, and optical properties, *Sol. Energy*, 2023, **259**, 107, DOI: 10.1016/j.solener.2023.05.015.

83 M. Li, F. Liu, J. P. Cheng, J. Ying and X. B. Zhang, Enhanced performance of nickel–aluminum layered double hydroxide nanosheets/carbon nanotubes composite for supercapacitor and asymmetric capacitor, *J. Alloys Compd.*, 2015, **635**, 225, DOI: 10.1016/j.jallcom.2015.02.130.

84 F. Nasirpouri, K. Alipour, F. Daneshvar and M. R. Sanaeian, Electrodeposition of anticorrosion nanocoatings, *Corrosion Protection at the Nanoscale*, 2020, pp. 473–497, DOI: 10.1016/B978-0-12-819359-4.00024-6.

85 M. W. Losey, J. J. Kelly, N. D. Badgayan, S. K. Sahu and P. R. Sreekanth, *Electrodeposition Reference Module in Materials Science and Materials Engineering*, 2017, DOI: 10.1016/B978-0-12-803581-8.10137-7.

86 D. S. Jayakrishnan, Electrodeposition: the versatile technique for nanomaterials, *Corrosion protection and control using nanomaterials*, 2012, vol. 86, pp. 86–125, DOI: 10.1533/9780857095800.1.86.

87 D. Zhang, M. Zhao, H. Zhang, M. Terrones and Y. Wang, A novel electro-synthesis of hierarchical Ni–Al LDH nanostructures on 3D carbon nanotube networks for hybrid-capacitors, *Carbon*, 2023, **201**, 1081–1089, DOI: 10.1016/j.carbon.2022.10.021.

88 M. Zhao, H. Zhang, S. Zhai, L. Sun, Z. Huang, M. Guo, Y. Liu, D. Zhang, M. Terrones and Y. Wang, Coaxial fabrication of Ni–Co layered double hydroxide into 3D carbon nanotube networks for high-performance flexible fiber supercapacitors, *J. Alloys Compd.*, 2022, **909**, 164664, DOI: 10.1016/j.jallcom.2022.164664.

89 F. Zhu, W. Liu, Y. Liu and W. Shi, Construction of porous interface on CNTs@NiCo-LDH core-shell nanotube arrays for supercapacitor applications, *J. Chem. Eng.*, 2020, **383**, 123150, DOI: 10.1016/j.cej.2019.123150.

90 A. Asatekin, M. C. Barr, S. H. Baxamusa, K. K. Lau, W. Tenhaeff, J. Xu and K. K. Gleason, Designing polymer surfaces *via* vapor deposition, *Mater. Today*, 2010, **13**, 26–33, DOI: 10.1016/S1369-7021(10)70081-X.

91 M. Sotelo-Lerma, R. A. Zingaro and S. J. Castillo, Preparation of CdTe coatings using the chemical deposition method, *J. Organomet. Chem.*, 2001, **623**, 81–86, DOI: 10.1016/S0022-328X(00)00597-0.

92 R. S. Mane and C. D. Lokhande, Chemical deposition method for metal chalcogenide thin films, *Mater. Chem. Phys.*, 2000, **65**, 1–31, DOI: 10.1016/S0254-0584(00)00217-0.

93 H. Chenn, F. Cai, Y. Kang, S. Zeng, M. Chen and Q. Li, Facile assembly of Ni–Co hydroxide nanoflakes on carbon nanotube network with highly electrochemical capacitive performance, *ACS Appl. Mater. Interfaces*, 2014, **6**, 19630–19637, DOI: 10.1021/am5041576.

94 R. I. Walton, Subcritical solvothermal synthesis of condensed inorganic materials, *Chem. Soc. Rev.*, 2002, **31**, 230–238, DOI: 10.1039/B105762F.

95 J. Lai, W. Niu, R. Luque and G. Xu, Solvothermal synthesis of metal nanocrystals and their applications, *Nano Today*, 2015, **10**, 240–267, DOI: 10.1016/j.nantod.2015.03.001.

96 O. A. Nerushev, M. Sveningsson, L. K. Falk and F. Rohmund, Carbon nanotube films obtained by thermal chemical vapour deposition, *J. Mater. Chem.*, 2001, **11**, 1122–1132, DOI: 10.1039/B009775F.

97 G. D. Nessim, Properties, synthesis, and growth mechanisms of carbon nanotubes with special focus on thermal chemical vapor deposition, *Nanoscale*, 2010, **2**, 1306–1323, DOI: 10.1039/B9NR00427K.

98 X. Li, J. Shen, W. Sun, X. Hong, R. Wang, X. Zhao and X. Yan, A super-high energy density asymmetric supercapacitor based on 3D core–shell structured NiCo-layered double hydroxide@carbon nanotube and activated polyaniline-derived carbon electrodes with commercial level mass loading, *J. Mater. Chem.*, 2015, **3**, 13244–13253, DOI: 10.1039/C5TA01292A.

99 A. Lee, M. Vörös, W. M. Dose, J. Niklas, O. Poluektov, R. D. Schaller, H. Iddir, V. A. Maroni, E. Lee, B. Ingram and L. A. Curtiss, Photo-accelerated fast charging of lithium-ion batteries, *Nat. Commun.*, 2019, **10**, 4946, DOI: 10.1038/s41467-019-12863-6.

100 S. I. Fletcher, F. B. Sillars, R. C. Carter, A. J. Cruden, M. Mirzaeian, N. E. Hudson, J. A. Parkinson and P. J. Hall, The effects of temperature on the performance of electrochemical double layer capacitors, *J. Power Sources*, 2010, **195**, 7484–7488, DOI: 10.1016/j.jpowsour.2010.05.043.